COMPARISON OF X-RAY DEPOSITION CODES

Clifford E. Rhoades, Jr.
Ernest F. Plechaty
G. Richard Wirtenson
LLNL

William H. Childs
Aerospace Corporation

Alan J. Watts
Ktech Corporation

Milton Merker
S-Cubed, A Division of Maxwell Labs., Inc.

COMPARISON OF X-RAY DEPOSITION CODES*

Clifford E. Rhoades, Jr.
Ernest F. Plechaty
G. Richard Wirtenson
University of California
Lawrence Livermore National Laboratory
Livermore, CA 94550

William H. Childs
Aerospace Corporation
Los Angeles, CA 90009

Alan J. Watts
Ktech Corporation
Albuquerque, NM 87110

Milton Merker
S-Cubed, A Division of Maxwell Labs., Inc.
La Jolla, CA 92038

ABSTRACT

We present a comparison of three computer codes (GENRAT-DEAP, Aerospace Corporation; TFT, Ktech; and XRT, S-Cubed) designed to calculate the heating in thin layers caused by the deposition of X-rays. In addition to the X-ray deposition process, these codes treat the thermal and mechanical processes in different ways and to differing degrees of accuracy. There is an interest in identifying the relative accuracies of these codes in predicting the survivability of optical coatings subjected to intense X-ray fluxes. A few test cases of coatings design and X-ray fluences have been defined and run on each code. The results are presented and a comparison made for each design. As a benchmark for comparing the X-ray deposition part of each code, the Lawrence Livermore National Laboratory (LLNL) code TART has been run for the same data set. These results are also presented.

INTRODUCTION

In the preceding two papers, the effort to characterize optical surfaces by the Angular Resolved Scatterometer[1] and the experimental program[2] to understand the behavior of optical elements exposed to X-rays have been discussed. In this paper, our theoretical program to calculate the effects of X-rays on optical elements is presented. Specifically, we discuss a comparison of three computer codes designed to calculate the effects of the deposition of X-rays in thin layers. In addition to the work at the Lawrence Livermore National Laboratory, this paper involves efforts on the part of Aerospace Corporation (Los Angeles, CA), Ktech Corporation (Albuquerque, NM), and S-Cubed (La Jolla, CA). The three computer codes are GENRAT-DEAP[3-5], at Aerospace Corporation, TFT (Thin Film Transport)[6-8] at Ktech Corporation, and XRT (X-Ray Transport)[9-11] at S-Cubed. These three computer codes treat the X-ray deposition process, the resulting thermal behavior, and mechanical response in different ways, with different numerical techniques and to differing degrees of accuracy.

The present study investigates the relative accuracies of these codes in predicting the survivability of optical coatings exposed to intense X-ray fluences. This has been done by creating four model optical element designs of two distinct types and by taking three X-ray spectra of various fluences. Altogether, there are more than 100 calculations in the test suite discussed in this paper. For brevity, only a few calculations typical of the results of the comparison study are shown. As a benchmark for comparing the X-ray deposition part of each code, the Lawrence Livermore National Laboratory code TART[12,13] has also been run on the model problems.

To facilitate the comparison effort, the codes use the same physical data including cross sections and thermal conductivities as well as the same spatial and energy zoning to the maximum extent possible given the various code restrictions. While the same physical data were entered, there is no guarantee that identical data were employed during the calculations, since each code uses a different data interpolation scheme. In addition, some of the codes select their own zoning based on accuracy or other conditions and hence use of exactly identical zoning is not, strictly speaking, possible.

THE THREE CODES

For the sake of completeness, a brief description of the three computer codes is given in this section. For more detailed information, the reader is directed to the previously indicated references.

All three computer codes have two properties in common. They are all one dimensional in physical space. That is, they solve their physics equations in one spatial dimension, namely mirror thickness, and assume that the other two dimensions are large by comparison. In addition, the numerical schemes are all deterministic.

GENRAT-DEAP, having been developed in the early 1970s, is the oldest of the three computer codes. It is also the simplest of the three. It

incorporates the physics of X-ray deposition and that of thermal conduction. Secondary effects such as fluorescence and electron deposition are not included. The energy resulting from X-ray deposition is coupled immediately into the thermal electron sea and the time–dependent diffusion equation for thermal transport is solved with the corresponding sources. The equation for X-ray deposition is solved by a multigroup, finite element integration. The thermal conduction equation is solved by finite difference using an explicit three time–level, modified Du Fort Frankel method.

TFT is the newest of the three computer codes. It is a public domain code available through the United States Air Force. Development started in 1983 and continues at the present time. Consequently TFT has not been used by the community as much as the other two codes. TFT, however, is more robust in the physics it addresses than GENRAT–DEAP. Like XRT, it includes the physics of X-ray deposition, electron transport, thermal conduction and mechanical response. The calculation of heating caused by the deposition of X-rays and the resulting thermal and mechanical behavior represents a somewhat more complicated exercise than typical of most standard modeling efforts. The reasons for this are two–fold. First, the mean free path of photo and autoionization electrons is comparable to the thickness of the thin films and thus the deposition of electrons cannot be considered local. Second, thermal diffusivities have a significant density dependence and thus mechanical response couples strongly to thermal behavior. In TFT, the equation for X-ray deposition is solved by a multigroup forward–backward direction integration scheme. Electron transport is performed by an overlay of geometric isotropic distributions based on higher order Spencer solutions. Thermal conduction is provided by a one–dimensional explicit solution of the heat conduction equation. The equations for mechanical response are those of the Puff 74 code[14] which implements a standard von Neumann Richtmyer Brode explicit finite difference method.

XRT is perhaps the most commonly used of the three computer codes. Its development started in the late 1970s. Like many computer codes, it continues to undergo revisions and additions. The most recent include conversion to the Cray line of supercomputers and coupling to a Puff–like mechanical response code. XRT, like TFT, is more robust in the physics it addresses than GENRAT–DEAP. Specifically, it models in one spatial dimension the physics of X-ray deposition, electron transport, thermal conduction and mechanical response. As far as the physics is concerned, XRT and TFT are intended to address the same physical phenomena. They do differ in the details as well as in the numerical methods used. XRT handles X-ray deposition by multigroup discrete ordinates. It does electron transport by the method of characteristics, applied to a two–term spherical harmonics expansion approximation (P1) of the Spencer–Lewis electron transport equation. Thermal transport is obtained by a simple Richardson extrapolation of a fully implicit backward Euler solution of the heat conduction equation. The equations for mechanical response are handled by a Puff–like code which implements a standard von Neumann Richtmyer Brode explicit finite difference method.

THE MODEL PROBLEMS

Two different types of model problems are employed in the calculations described in this paper. As can be seen from their simplicity, they have been chosen strictly as model problems and are not intended as actual mirror designs. One type has a fused silica substrate of .5 cm with a beryllium energy sharing layer of 1000 nm and a reflective overcoating, either aluminum or gold, of 75 nm and 125 nm, respectively. The other consists of a heavy metal, either gold or molybdenum, substrate of .5 cm with an aluminum layer of 75 nm and an overcoating of aluminum oxide of 150 nm. There are, thus, a total of four model optical element designs. These are depicted in cross section in Fig. 1.

In addition to the model optical element designs, it is necessary to specify model spectra, fluence, pulse shape and duration. There are three basic types of model spectra – argon, monoenergetic and blackbody. The argon spectrum is a model of the output of the Blackjack V simulator at Maxwell Laboratories in San Diego. Its pulse has an isosceles triangular shape with a base of 28.6 ns. Three fluences, .1, .5, and .9 cal/cm^2, are employed in the calculations. For the monoenergetic spectra, no thermal calculations are intended. Hence, no fluence, pulse shape or duration are specified for them. Two blackbody spectra of 1 and 4 keV energy and .1 and .4 cal/cm^2 fluence, respectively, with a pulse duration of 10 ns are also used. For convenience, the model spectra are summarized in Table 1.

DATA AND PARAMETERS

The physical data used in this exercise are those of the bulk materials. In the real world, the properties appropriate to thin films, where they differ from bulk materials, must be used. These data have been mutually agreed upon as being suitable for the purpose of common input to the codes. We note that these data are not necessarily accurate. The choice and use of such data derive solely from expediency.

Thermophysical data for the six materials used in the model problems are those of Childs.[15,16] The specific properties are: 1. density (g/cm^3); 2. melting point (°C); 3. vaporization point (°C); 4. heat of fusion (cal/g); 5. heat of vaporization (cal/g); 6. heat capacity (cal/g-°C); and 7. thermal conductivity (cal/sec–cm–°C).

The argon spectrum used in the calculation is that defined by Merker[17] in 37 specified energy bins with a normalized fraction of fluence in each energy bin and an isosceles triangular time pulse of 28.6 ns. The 1 and 4 keV blackbody integral spectra in 109 energy bins are also provided by Childs.[18]

The X-ray interaction data, provided by Watts,[19] are those of Biggs and Lighthill.[20] Specific data include: 1. placement in energy of the primary lines (keV); 2. average K fluorescent energy (keV); and 3. photoelectric cross section. The Biggs and Lighthill X-ray interaction data are used in the GENRAT–DEAP, TFT, and XRT calculations. By contrast, TART calculations are based on the standard evaluated Livermore X-ray interaction data.[21]

Initially, the spatial zoning for the deposition phase of the calculations is taken as ten equal width zones within each film or substrate layer. For calculational purposes, the .5 cm substrate contains four layers of increasing thickness. Layer thicknesses are 1., 10., 100., and 4889 μm with the 1 μm thickness next to the film layer. Since each model mirror design has two films and a substrate of four layers, there are 60 zones in the calculations. An initial set of calculations with this zoning shows that this particular choice is marginal in the sense that not all of the calculations are converged. Subsequent calculations and most of the ones reported here have been made with twenty or more equal width zones for a total of 120 or more zones. The mechanical response calculations have been made with a 1000 or more zones.

The test set matrix of the calculations performed for the code comparison is shown in Table 2. The spectra are labeled by the letters A, B, and C across the top of Table 2. These letters identify the model spectra in Table 1 as given under the reference letter heading. The designs are labeled by the numbers 1, 2, 3, and 4 down the left hand side of Table 2. These numbers identify the model designs in Fig. 1. The presence of an "x" indicates that calculations are included in the test set. All cases have been run both with and without secondary effects, including fluorescence and electron production. Dose data have been compared for all cases. In addition, thermal and temperature data at the end of pulse have been calculated for the cases involving the argon and blackbody spectra. No thermal or temperature data have been computed for the monoenergetic spectra. Finally, mechanical response calculations have been performed only for design 1 exposed to a .9 cal/cm^2 fluence argon spectrum. Mechanical effects are often quite important in understanding mirror responses to X-ray fluences. Our choice of only one model mechanical response problem is due to the very long computer running times such calculations require.

RESULTS

Representative computational results are displayed in Fig. 2 through Fig. 28. Figures 2 through 11 contain the results for the argon spectrum calculations. Figures 12 through 16 contain the results for the monoenergetic deposition calculations. Figures 17 through 26 contain the results for the blackbody spectra calculations. Figures 27 and 28 contain the results of the mechanical response calculations. The formats for Figs. 27 and 28 are not the same as those for Figs. 2 through 26 and consequently they are discussed separately below.

Figures 2 through 26 have the following format. One of these quantities, either normalized dose (cm^2/g), enthalpy (cal/g) or temperature (°C), is plotted versus layer number. Within each layer number the scale is linear. However, the scale changes from one layer number to the next. For example, in Fig. 2, layer number 1 consists of 75 nm of aluminum while layer number 2 consists of 1000 nm of beryllium. Thus, the distance between the numbers 1 and 2 on Fig. 2 is 75 nm, while the distance between the numbers 2 and 3 is 1000 nm. To aid the reader, the thicknesses and compositions of these layers are displayed at the top of each figure below the caption.

Results in Figs. 2 through 26 are displayed in the following systematic fashion. The first group of figures contains the calculations without secondary efforts. These calculations are those of GENRAT/DEAP, TFT, XRT and TART. The second group of figures contains the calculations with secondary efforts. These calculations are those of TFT and XRT. Since GENRAT/DEAP and TART do not, in general, include secondary effects. However, it should be noted that TART calculations always include fluorescence but do not include the effects of secondary electrons. In temperature and enthalpy plots, the fluence level in cal/cm^2 is included in the caption. For monoenergetic and blackbody spectra, the energy is also included in the caption.

Figures 27 and 28 contain the results of the mechanical response calculation of design 1 exposed to an argon spectrum at .9 cal/cm^2 fluence. They include only TFT and XRT results, since GENRAT/DEAP and TART do not include the necessary physics. Unlike Figs 2 through 26, the stress (kbars) in Fig. 27 is displayed in a linear scale in distances from the mirror surface. Figure 27 is a snapshot in time. For the TFT calculation, the time is 15 ns. For the XRT calculation the time is 17 ns. In spite of the slight difference in time, the two calculations are in remarkable agreement. Indeed the XRT computation has propagated the pulse a somewhat further distance as one would expect. Figure 28 contains a plot of stress (kbars) versus time (ns) at a specific position within the mirror. For the TFT calculation, the position is 594 nm into the substrate. For the XRT calculation, the position is 954 nm into the substrate. The noise in the TFT calculation is believed to be the result of modeling the triangular time pulse of the argon spectrum with 24 histograms, combined with the signal reflection/transmission at each interface where an impedance mismatch occurs. In spite of the difference in position, the two calculations are in close agreement when one does a time filtering of the TFT results. Indeed, the XRT calculation being further from the front mirror surface lags somewhat behind in time when compared with the TFT calculation. This is exactly what one would expect physically.

CONCLUSIONS

Based on the previously displayed results, we make the following observations. Once adequate spatial zoning is used and proper boundary conditions in the substrate are taken, the four computer codes are in extremely good agreement for the deposition part of the calculations. In the deposition calculations, the complicated nature of the blackbody, and argon spectra overwhelm any differences in methods or data. Consequently, the monoenergetic spectra model problems are vital to understanding computer code and data differences. For example, in runs where no secondary effects are to be included, we clearly see that fluorescence has been included in the XRT and TART calculations. This explains the differences between XRT and TART on the one hand and GENRAT/DEAP and TFT on the other, as displayed in Fig. 14, because fluorescence is an important effect in gold at 20 keV. It is also evident that the X-ray interaction data and use in the four codes are not identical. These cause a factor of 5 difference in dose, for example, in placement of the K-edge in molybdenum at 20 keV. Use as reflected in the interpolation scheme also causes a few percent difference. Although there are minor differences in X-ray dose calculations, none are large.

By contrast, there are large thermal and temperature differences which cannot be explained by the differences in dose. These differences are substantial in gold, while less so in molybdenum. There is reasonable agreement with fused silicon, however. We believe that these differences are largely caused by the methods used to treat the melting phenomenon in the various codes. Additional work is underway to verify these observations. The treatment of secondary electron production transport and deposition clearly differs between XRT and TFT. The differences are especially noticeable at the interface between a heavy metal such as gold and a light metal such as aluminum. Some preliminary calculations with the TIGERP electron photon Monte Carlo code which is expected to be valid only for energies above 1 keV are inconclusive. Results for 50 keV photon energy are similar to those of XRT whereas results at 20 keV lie half-way between those of TFT and XRT. We are currently investigating the sources of these differences. Finally, mechanical response calculations provided by TFT and XRT are quite similar where the dose and thermal calculations are also similar.

For those concerned with designing survivable optics, we recommend the use of more than one code to calculate any specific design in a given environment. Additional work in tracking down the differences in secondary electron effects, for example, by inventing monoenergy electron dose problems, should be undertaken. Likewise, the thermal and temperature differences need to be fully understood. Finally, the optics community needs to have in place a scheme for providing evaluated physical data including X-ray interaction and thermophysical parameters which are valid for thin films. The data interpolation schemes should also be formally evaluated, approved and standardized.

ACKNOWLEDGMENTS

REFERENCES

1.   D. F. Edwards, C. H. Gillespie and G. R. Wirtenson, "Characterization of Optical Surface Degradation: The Angular Resolved Scatterometer (ARS)," **Proc. of the High Power Laser Optical Components Conf.** 29–31 October 1986, National Bureau of Standards, Boulder, CO.

2.   G. R. Wirtenson, D. F. Edwards, and T. T. Saito, "Test Results for Nuclear Hardened Optical Coatings," **Proc. of the High Power Laser Optical Components Conf.** 29–31 October 1986, National Bureau of Standards, Boulder, CO.

3.   W. H. Childs, "GENRAT-DEAP," private communications, 1986.

4. E. H. Fletcher, <u>Deposition of Radiation in Solids</u>, Aerospace Corporation, Los Angeles, CA, ATM 68(3250–30)–1 (1967).

5. B. J. McFarland, <u>Differential Equation Analyzer Program, Volume 1</u>, Advanced Systems Department, 589, Rocketdyne, Los Angeles, CA, LAP–69–552(RC) (1969).

6. A. J. Watts, <u>Thin Film Computer Code Development. The TFT Routine – Thin Film Transport: Part I – Background and Theory</u>, Ktech Corporation, Albuquerque, NM, Ktech TR 83–19 (1984).

7. A. J. Watts, C. M. Breen, and S. K. Sauer, <u>Thin Film Computer Code Development. The TFT Routine – Thin Film Transport: Part II – Thermal Conduction and Stress Response</u>, Ktech Corporation, Albuquerque, NM, Ktech TR 86–04 (1986).

8. A. J. Watts, C. M. Breen, and S. K. Sauer, <u>Thin Film Computer Code Development. Part III – PUFF TFT – A Material Response Computer Code Users Manual and Subroutine Descriptions</u>, Ktech Corporation, Albuquerque, NM, Ktech TR 85–16 (1986).

9. J. R. Triplett, <u>The XRT Code</u>, S–Cubed, La Jolla, CA, SSS–R–83–5829 (1982).

10. J. R. Triplett, B. Shkoller, M. H. Rice, S. Shkoller, and M. Merker, <u>XRTH, A Combination of XRT and Hydro Codes</u>, S–Cubed, La Jolla, CA, SSS–R–86–7981 (1986).

11. J. R. Triplett, B. Shkoller, and M. Merker, <u>XRTH Users Manual and Reference Guide</u>, S–Cubed, La Jolla, CA, SSS–R–87–8420 (1986).

12. E. F. Plechaty and J. R. Kimlinger, <u>TART–NP: A Coupled Neutron–Photon Monte Carlo Transport Code</u>, Lawrence Livermore National Laboratory, Livermore, CA, UCRL–50400, Vol. 14 (1976).

13. J. R. Kimlinger and E. F. Plechaty, <u>TART and ALICE Input Manual</u>, Lawrence Livermore National Laboratory, Livermore, CA, UCID–17026, Rev. 2 (1986).

14. R. Cecil, C. D. Newlander, and R. T. Scannon, <u>PUFF74 – Material Response Computer Code</u>, Air Force Weapons Laboratory, Kirtland AFB, NM, AFWL–TR–76–43, Vols. I and II (1977).

15. W. H. Childs, <u>Thermophysical Properties of Selected Space–Related Materials</u>, Aerospace Corporation, Los Angeles, CA, TOR–0086 (6435–02)–1 Vol. 1 (1981).

16. W. H. Childs, <u>Thermophysical Properties of Selected Space–Related Materials</u>, Aerospace Corporation, Los Angeles, CA, TOR–0086 (6435–02)–1 Vol. 2 (1986).

17. M. Merker, private communication, 4 June 1986.

18. W. H. Childs, private communication, 10 June 1986.

19. A. J. Watts, private communication, 12 June 1986.

20. F. Biggs and R. Lighthill, <u>Analytical Approximations for X-ray Cross Sections II</u>, Sandia National Laboratories, Albuquerque, NM, SC-RR-71 0507 (1971).

21. E. F. Plechaty, D. E. Cullen, and R. J. Howerton, <u>Tables and Graphs of Photon-Interactions Cross Sections from 0.1 keV to 100 MeV Derived from the LLL Evaluated-Nuclear-Data Library</u>, Lawrence Livermore National Laboratory, Livermore, CA, UCRL-50400, Vol 6, Rev. 3 (1981).

TABLE 1. Model problem spectra.

Type	Pulse Duration	Fluence (cal/cm^2)	Reference Letter
Argon	28.6 ns	0.1, 0.5, and 0.9	A
Monoenergetic (0.5, 1.0, 2.0, 5.0, 10.0, 20.0 and 50 keV)			B
1 and 4 keV Blackbody	10 ns	0.1 and 0.4 respectively	C

TABLE 2. Test set matrix.

Design	Spectra A	Spectra B	Spectra C
1	X	X	X
2		X	X
3		X	X
4	X	X	X

All cases run with and without secondary effects. All cases provide dose data. A and C include temperature at end of pulse. No temperature data for B.
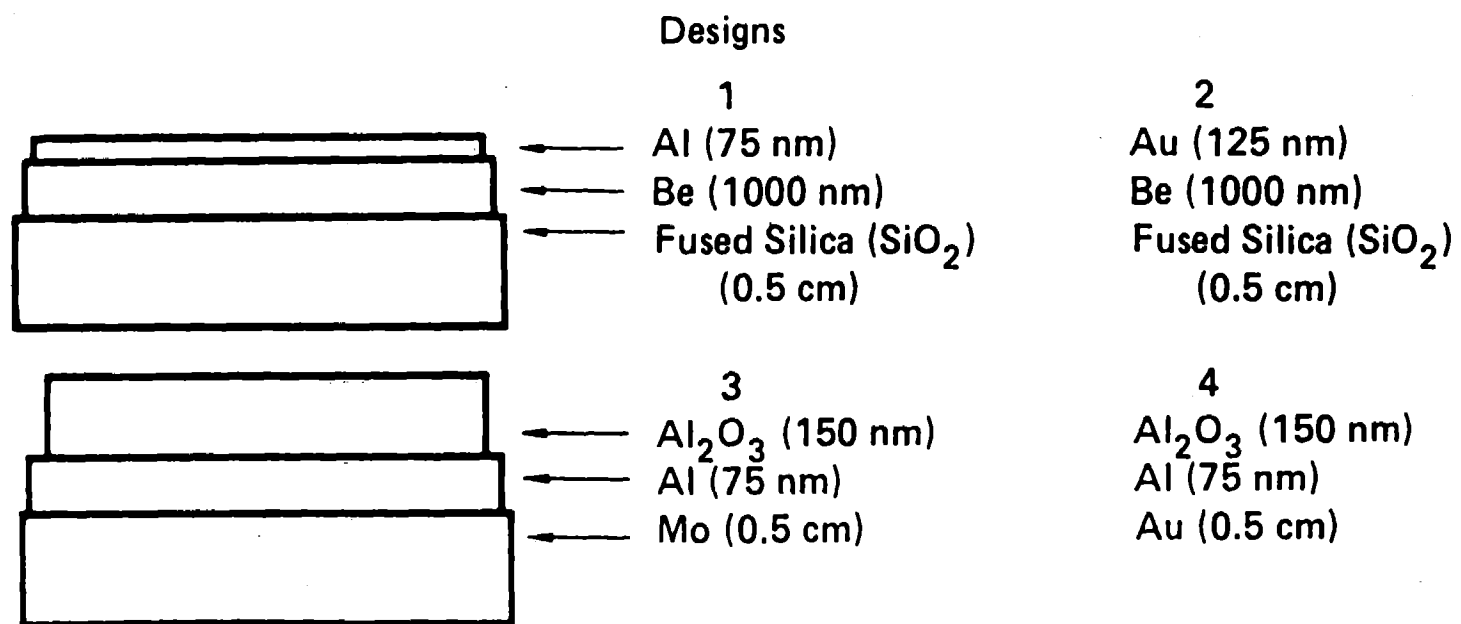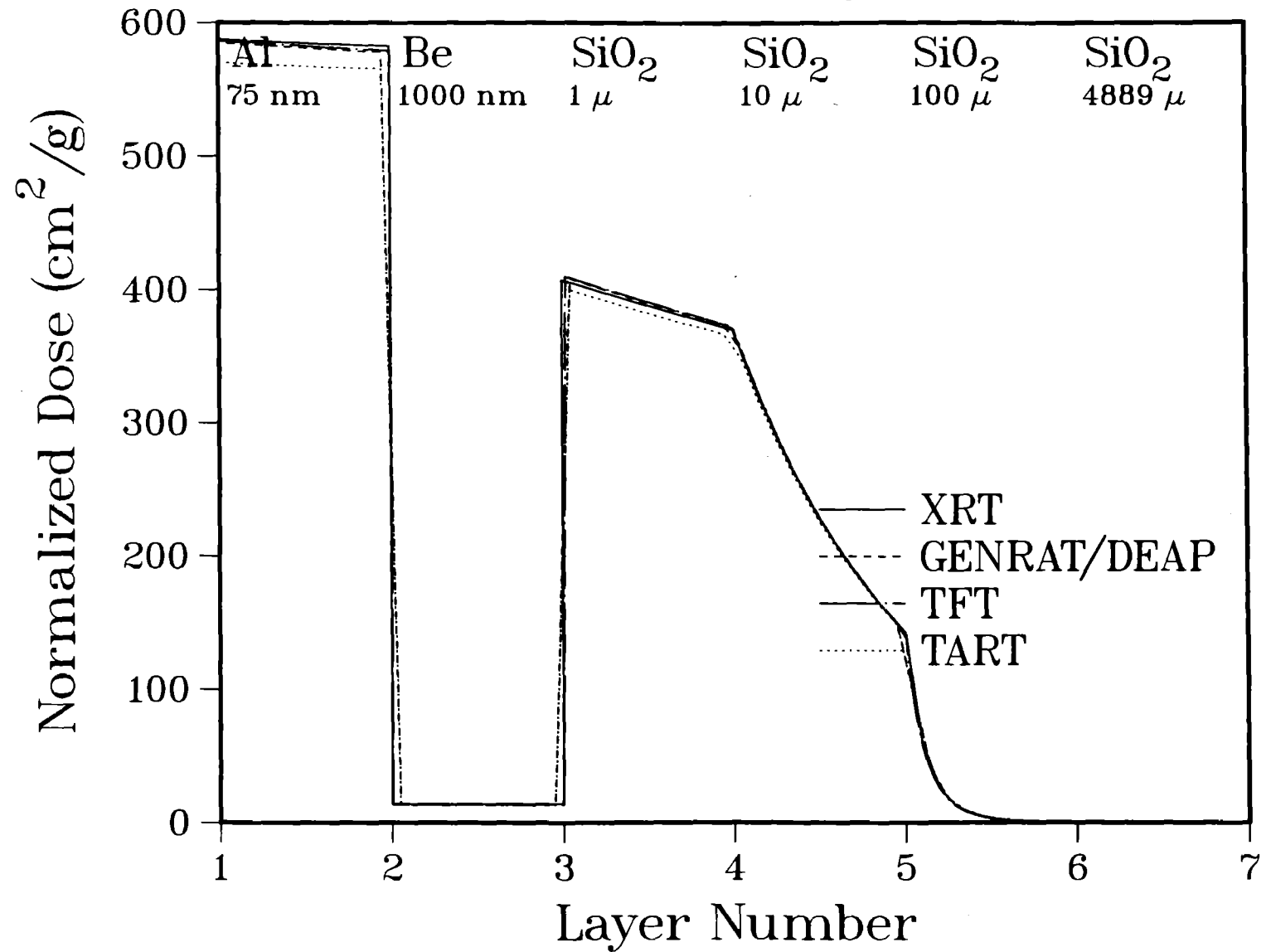
Designs

1

AI (75 nm)
Be (1000 nm)
Fused Silica (SiO$_2$)
(0.5 cm)

2

Au (125 nm)
Be (1000 nm)
Fused Silica (SiO$_2$)
(0.5 cm)

3

Al$_2$O$_3$ (150 nm)
AI (75 nm)
Mo (0.5 cm)

4

Al$_2$O$_3$ (150 nm)
AI (75 nm)
Au (0.5 cm)

FIGURE 1

Argon

Without Secondary Effects

FIGURE 2

Argon
Fluence = 0.1 cal/cm^2
Without Secondary Effects

Enthalpy (cal/g) – End of Pulse

| Al | Be | SiO$_2$ | SiO$_2$ | SiO$_2$ | SiO$_2$ |
| 75 nm | 1000 nm | 1 μ | 10 μ | 100 μ | 4889 μ |

—— XRT
- - - TFT

Layer Number

FIGURE 3

– 12 –
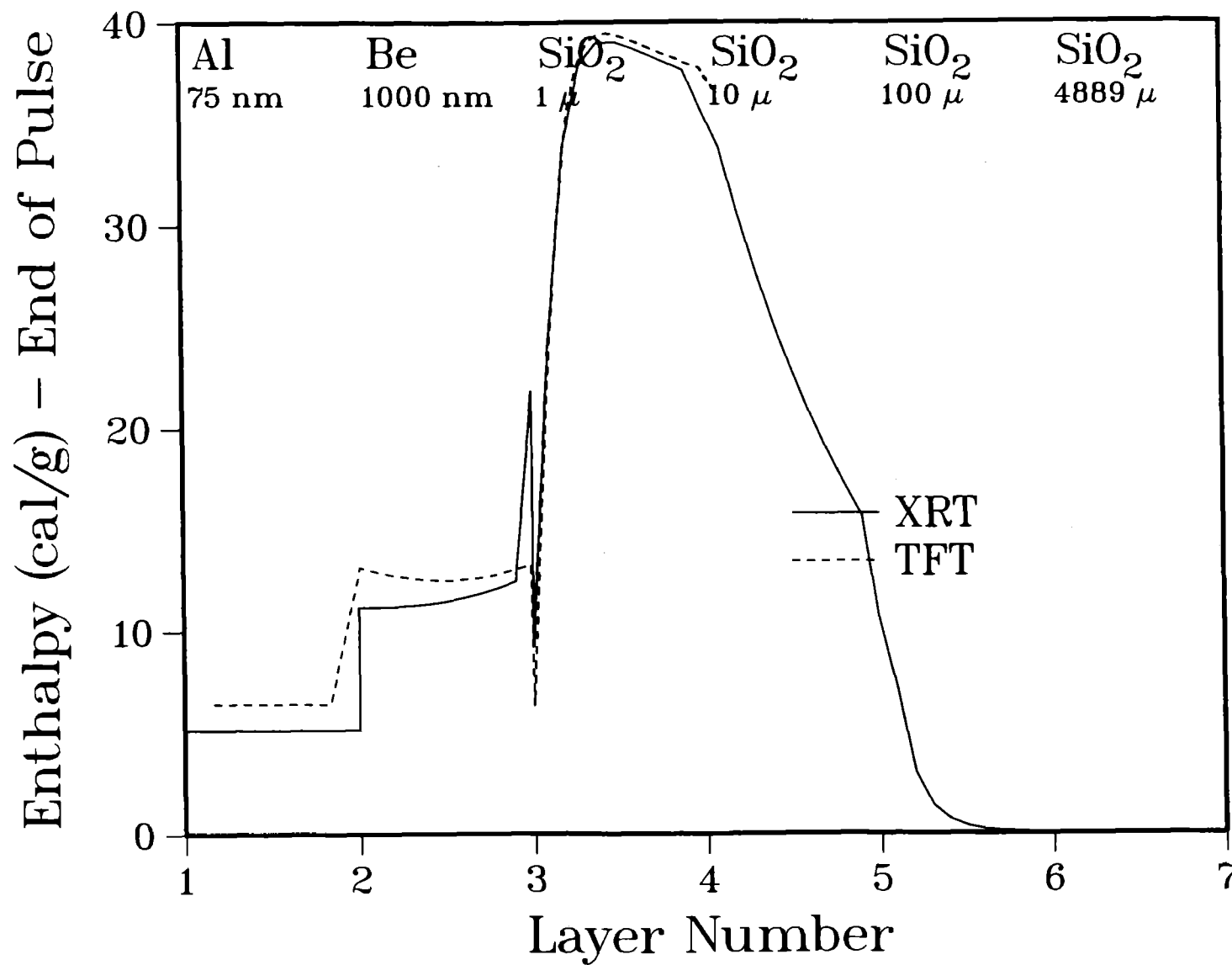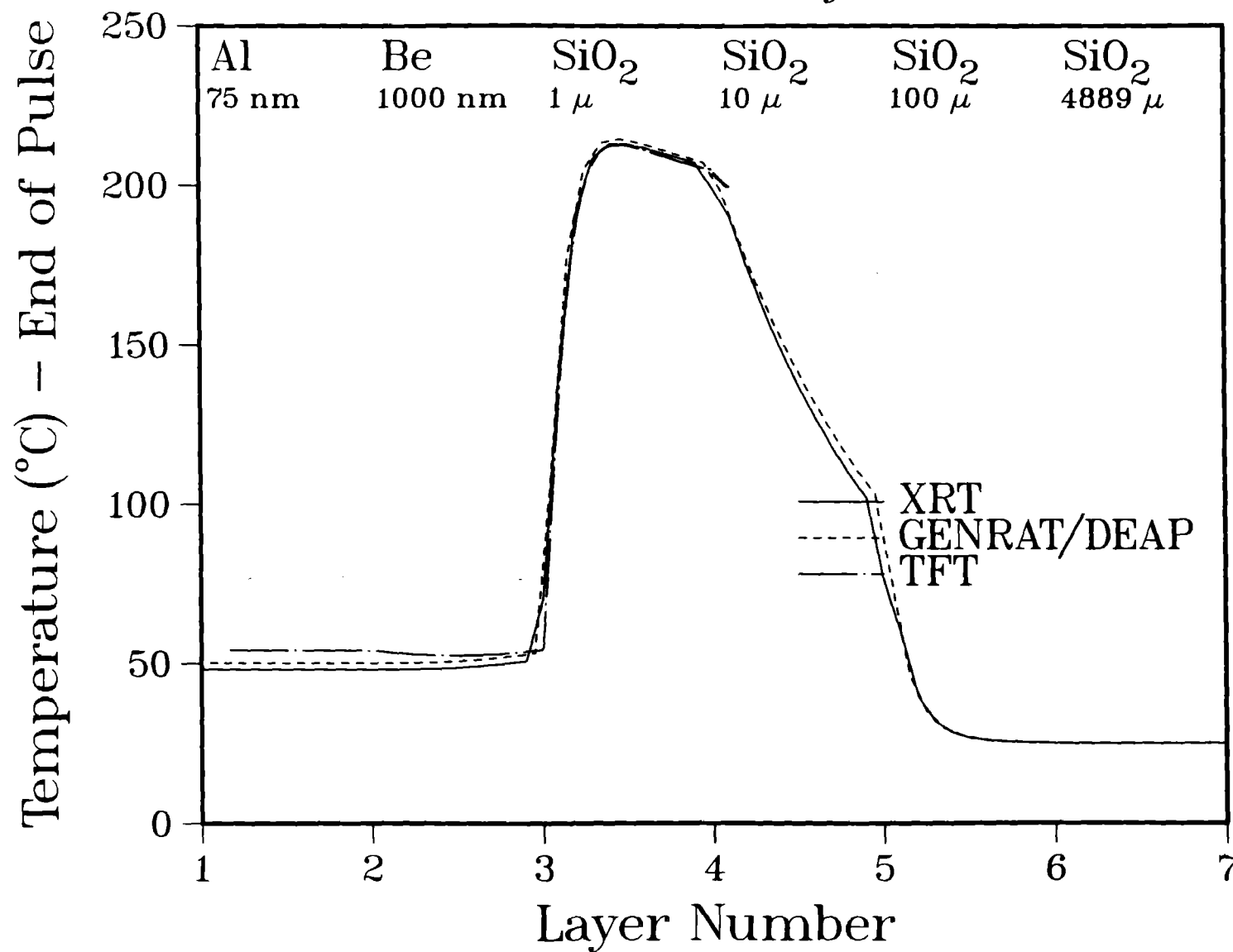
FIGURE 4

Argon

With Secondary Effects

FIGURE 5

– 14 –
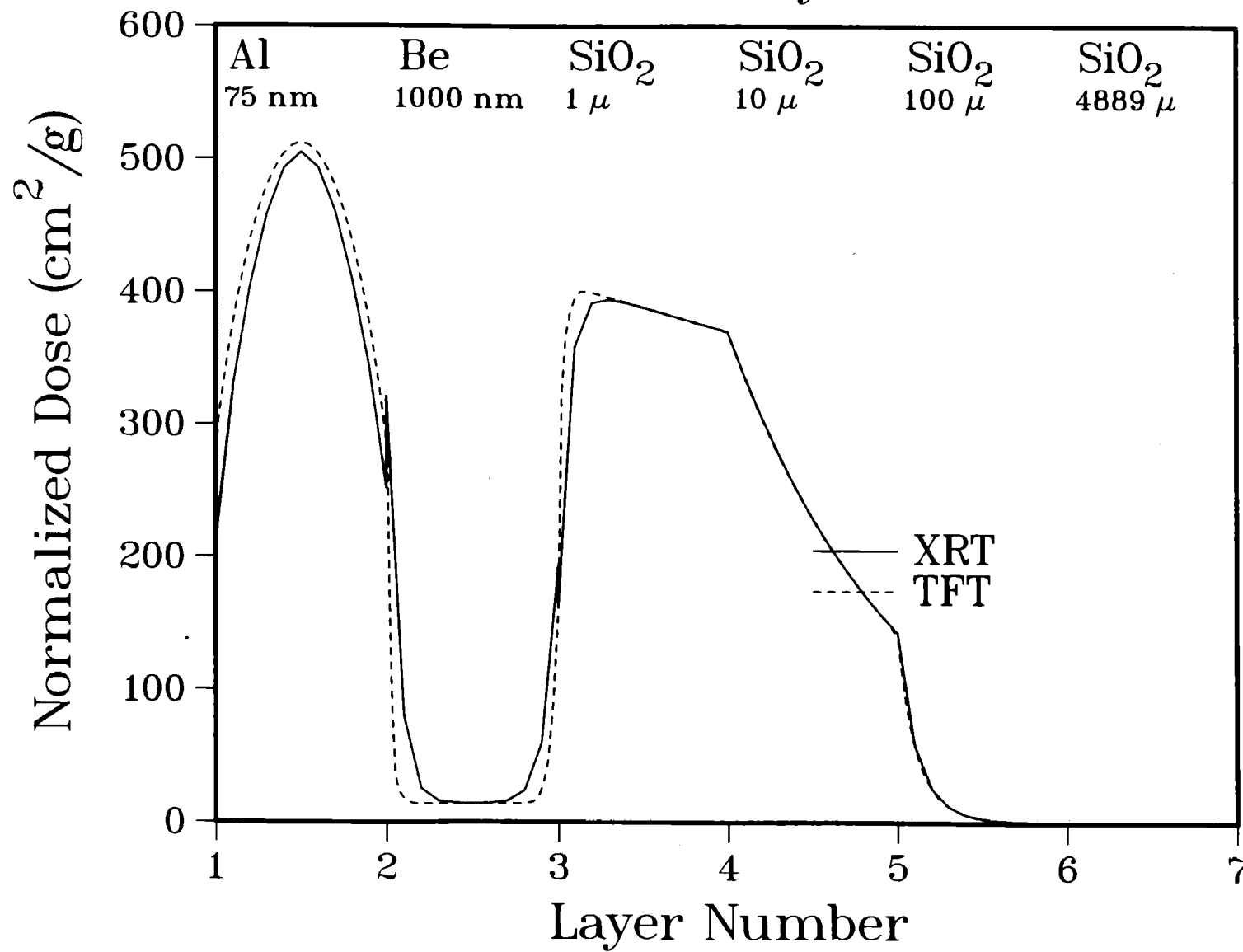
Argon
Fluence = 0.1 cal/cm^2
With Secondary Effects

FIGURE 6

– 15 –
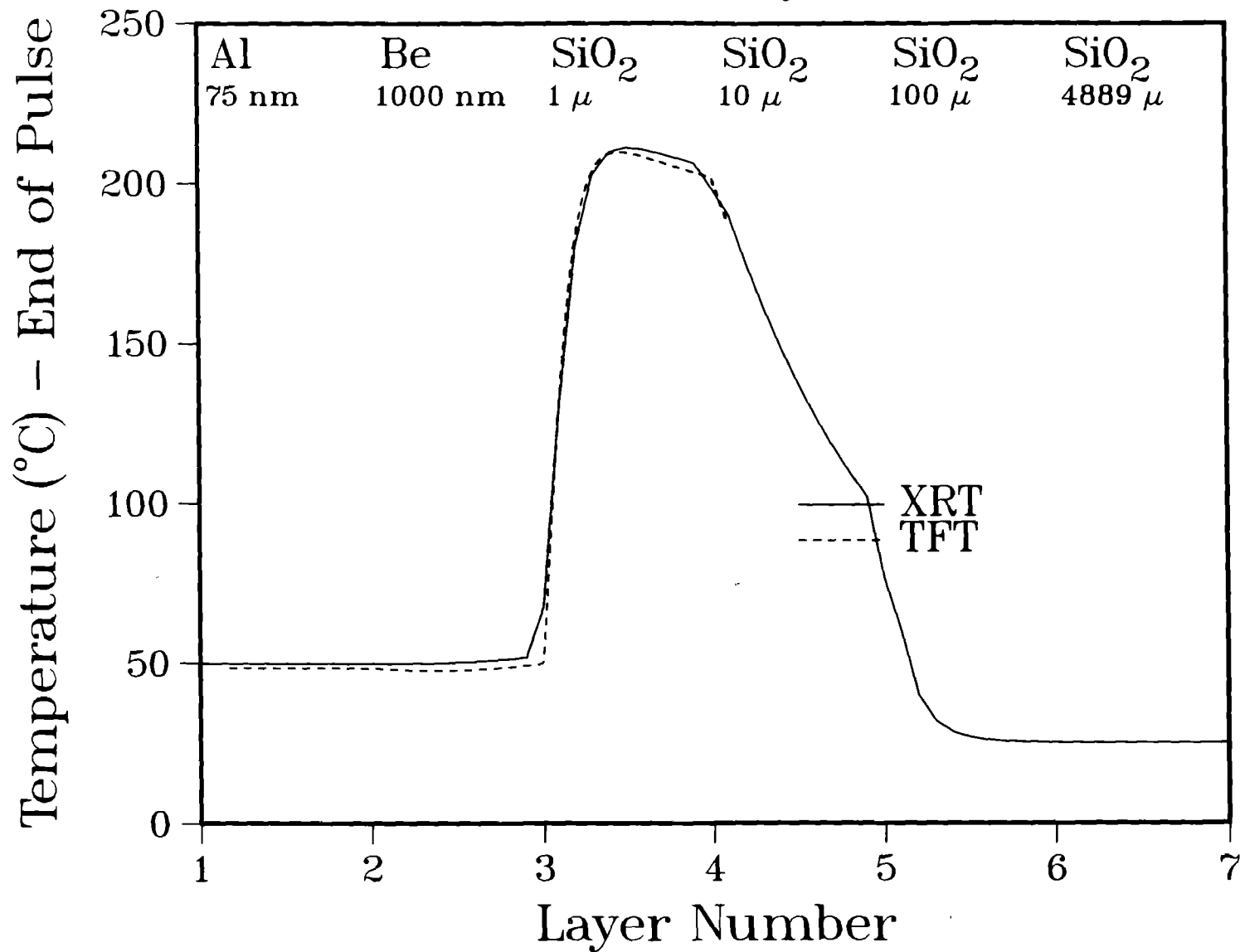
Argon

Without Secondary Effects
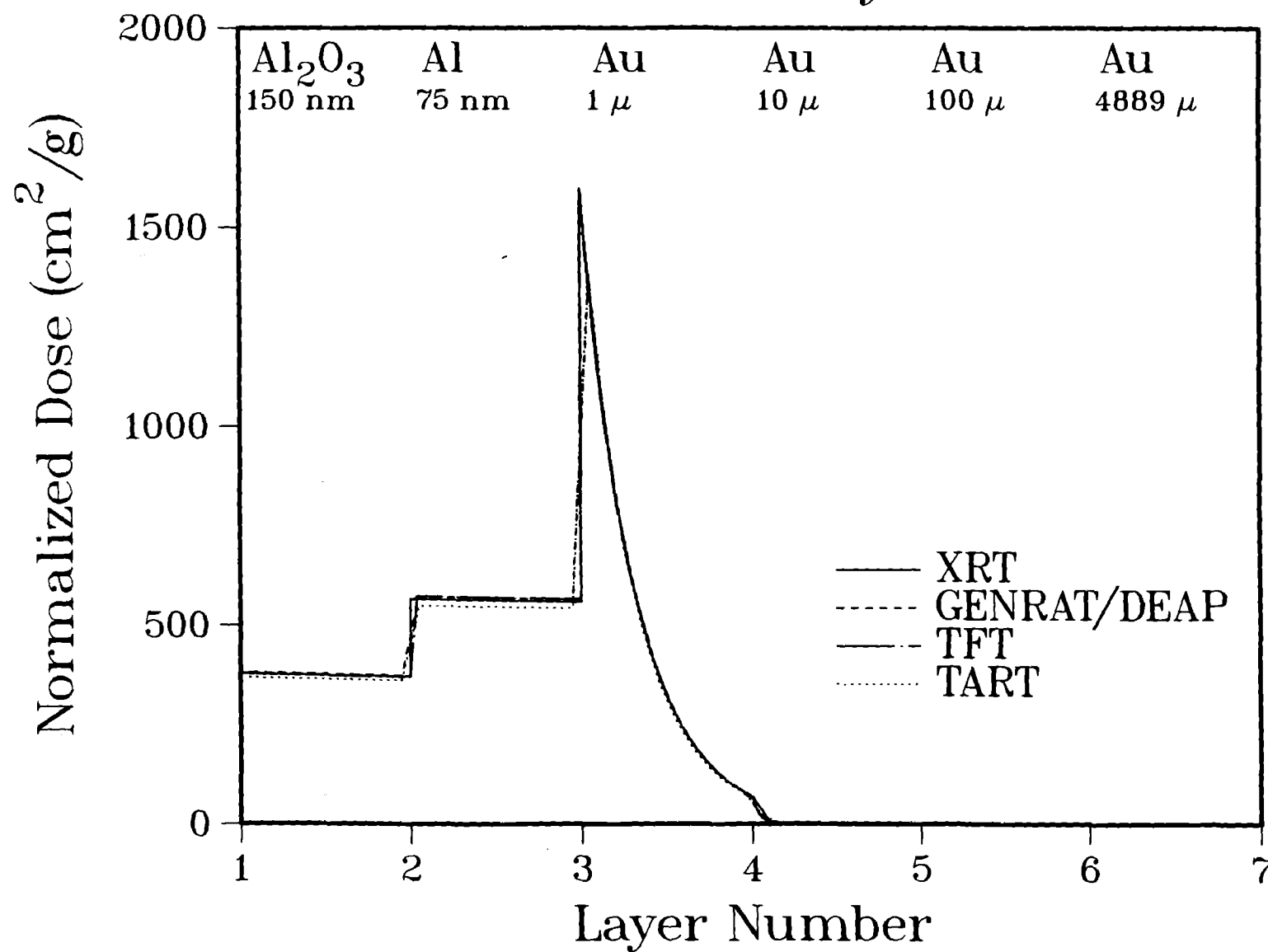
FIGURE 7

Argon
Fluence = 0.1 cal/cm^2
Without Secondary Effects
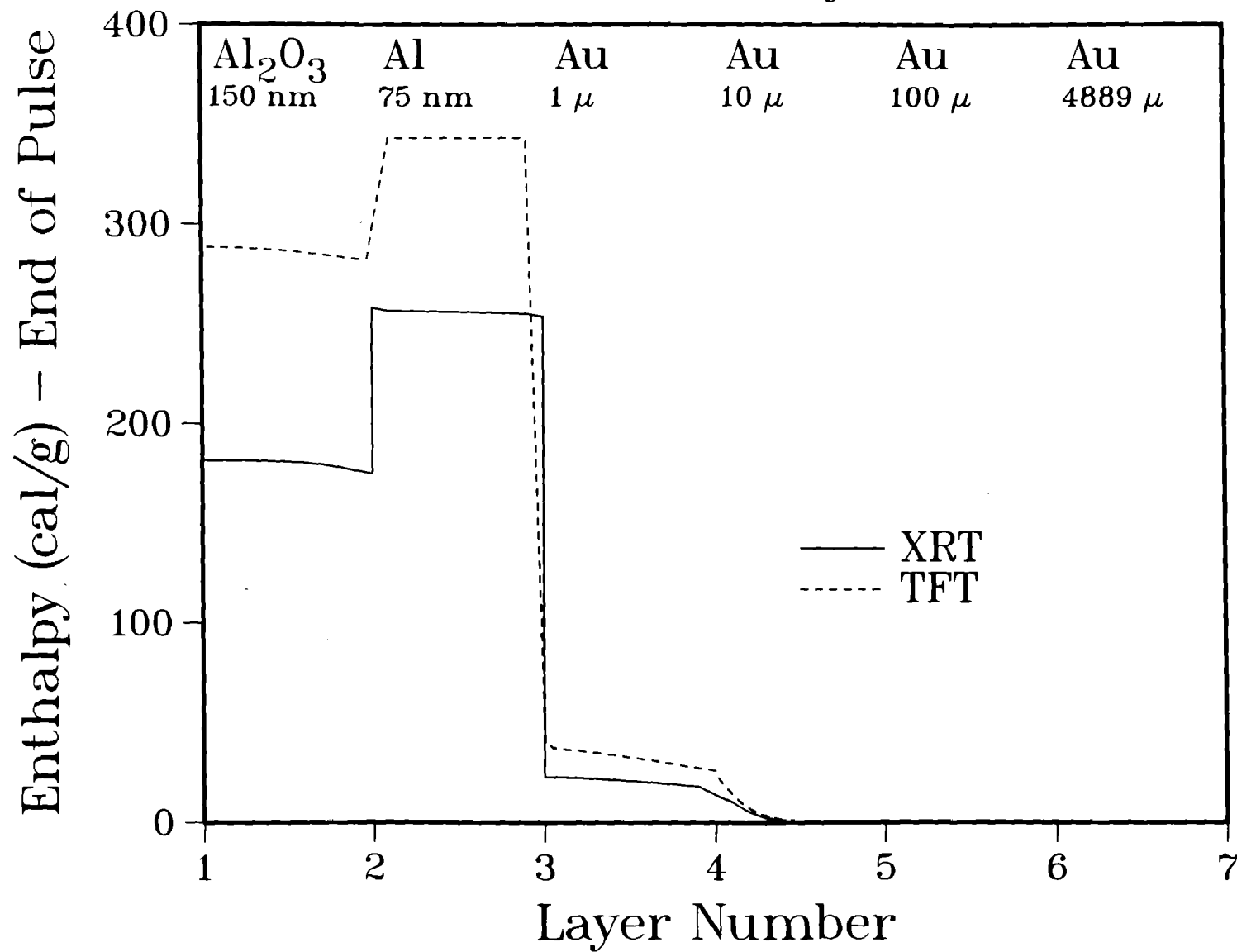
FIGURE 8

Argon
Fluence = 0.1 cal/cm^2
Without Secondary Effects

FIGURE 9
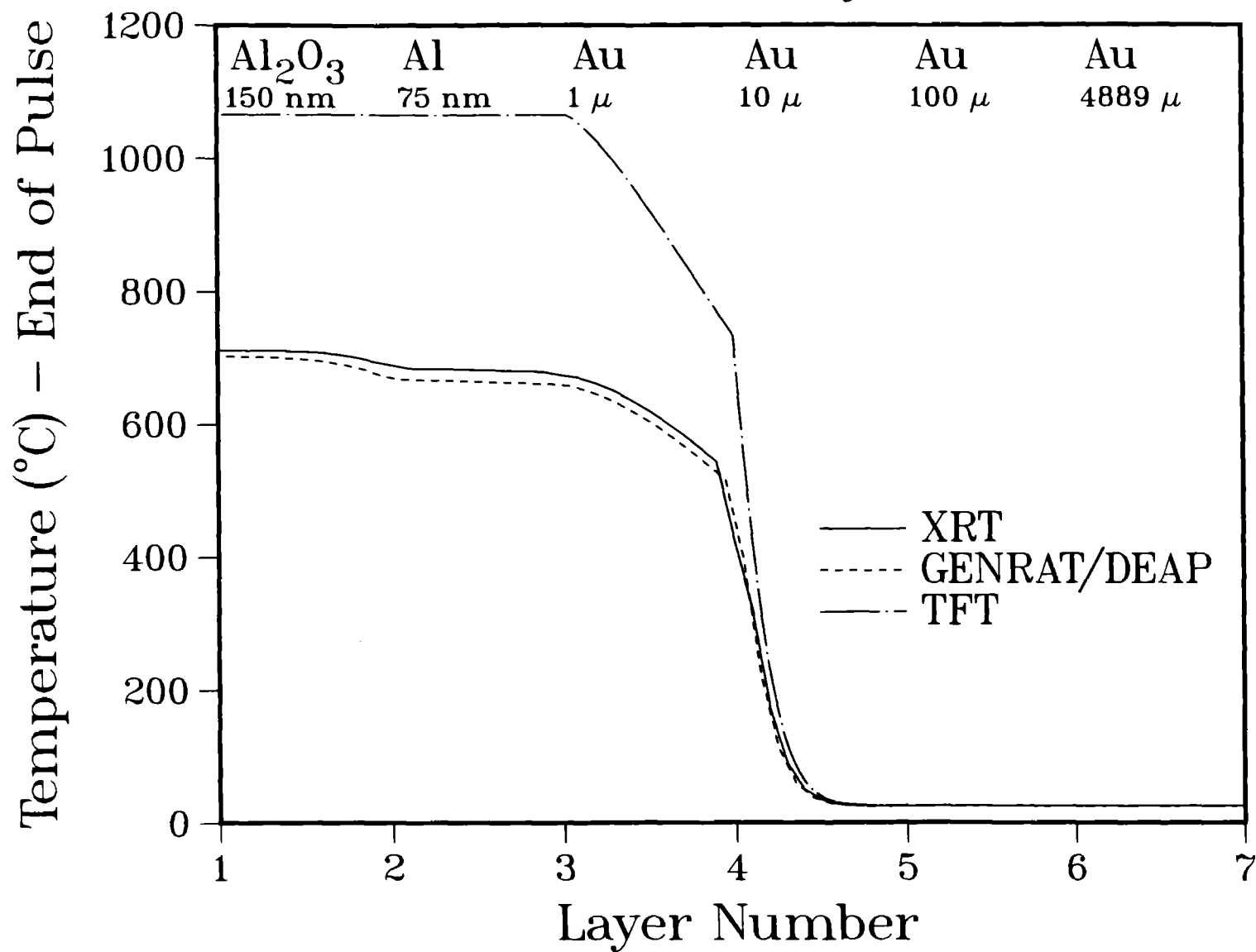
Argon

With Secondary Effects
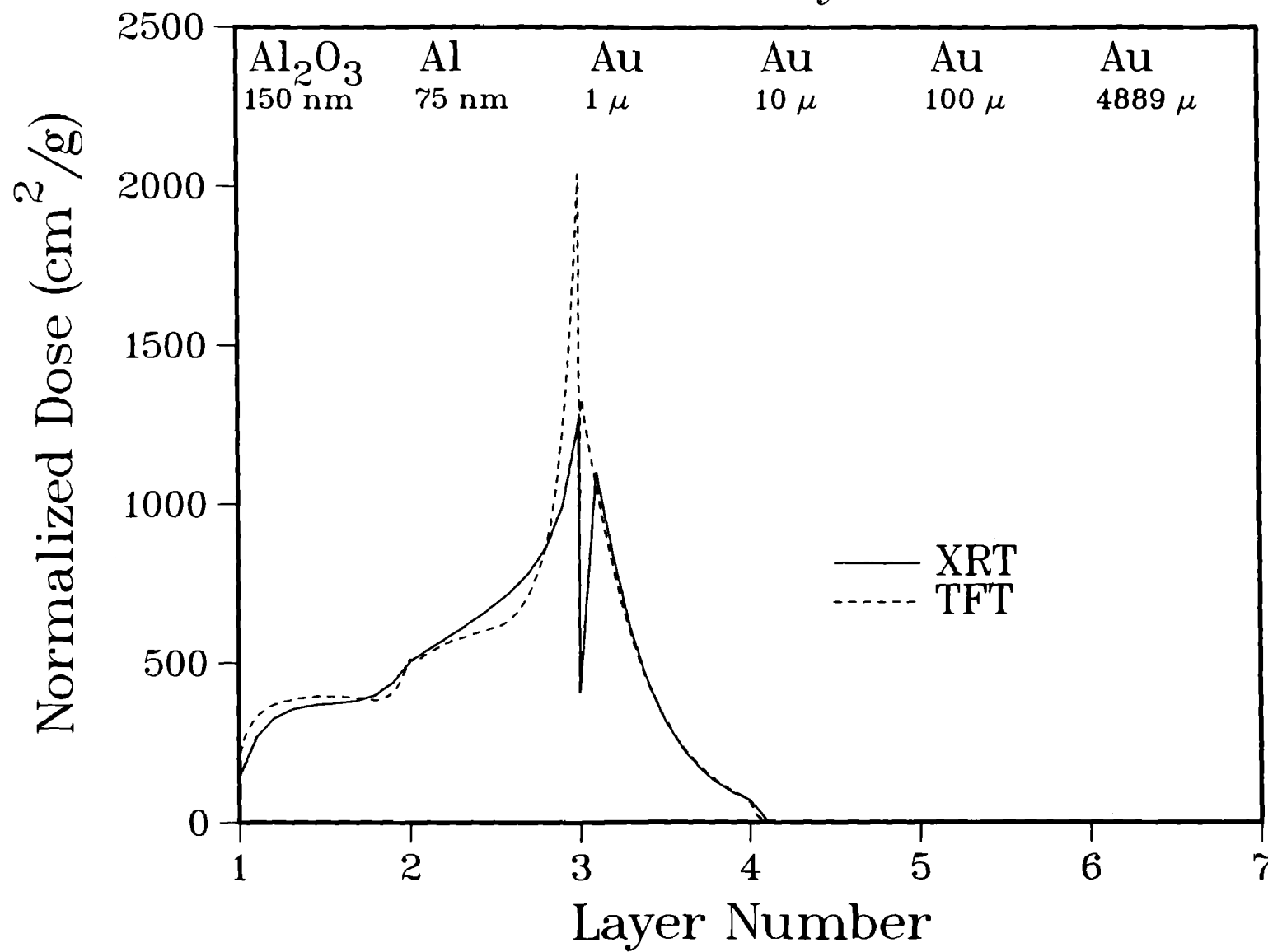
FIGURE 10

Argon
Fluence = $0.1 \; \mathrm{cal/cm}^2$
With Secondary Effects

FIGURE 11

– 20 –

FIGURE 12

B1A
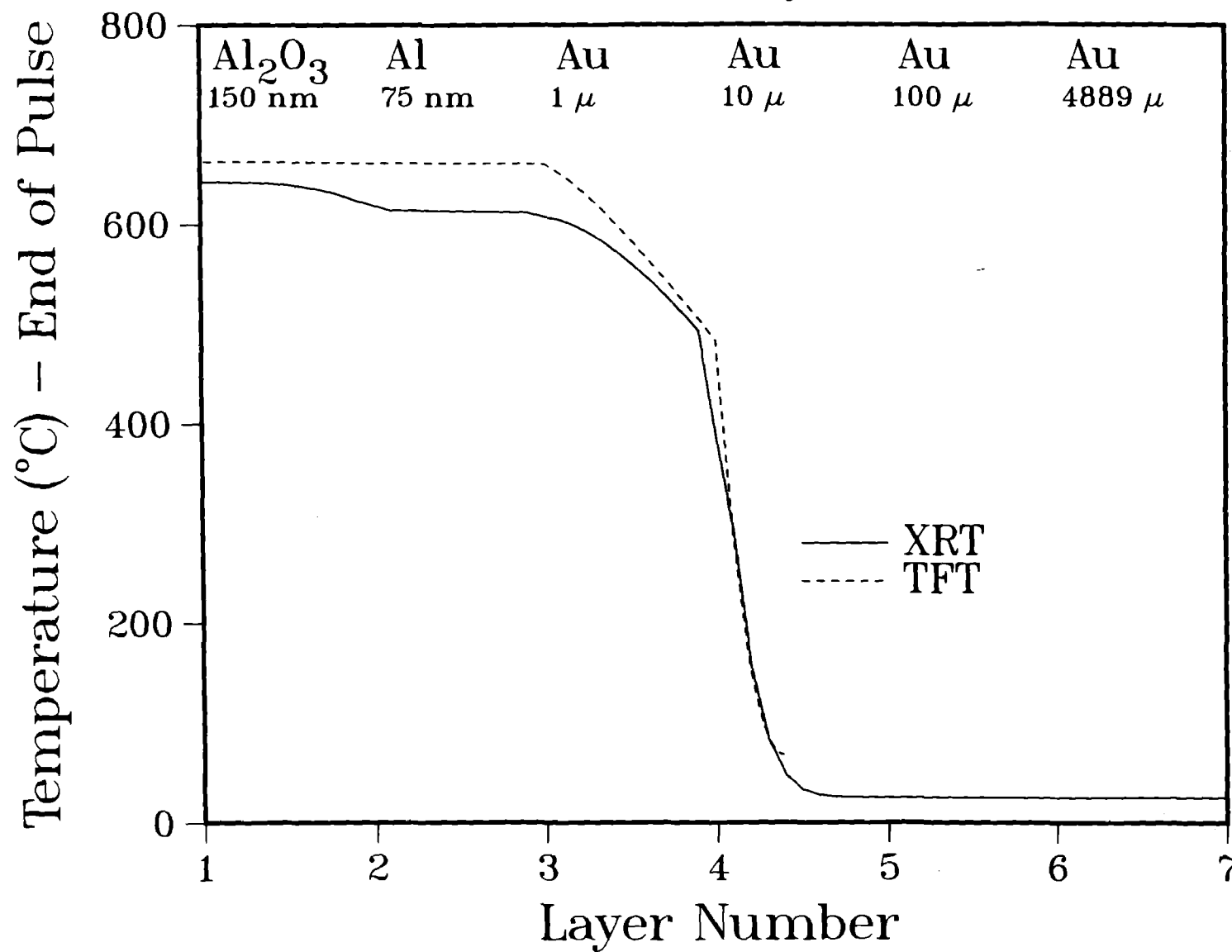
Mono–Energetic   0.5 keV

Without Secondary Effects

Al	Be	SiO_2	SiO_2	SiO_2	SiO_2
75 nm	1000 nm	1 μ	10 μ	100 μ	4889 μ

Normalized Dose (cm^2/g)

8000

6000

4000

2000

0

——— XRT
- - - - GENRAT/DEAP
—·- TFT
········· TART

1   2   3   4   5   6   7

Layer Number

B1A   Mono–Energetic   0.5 keV

With Secondary Effects
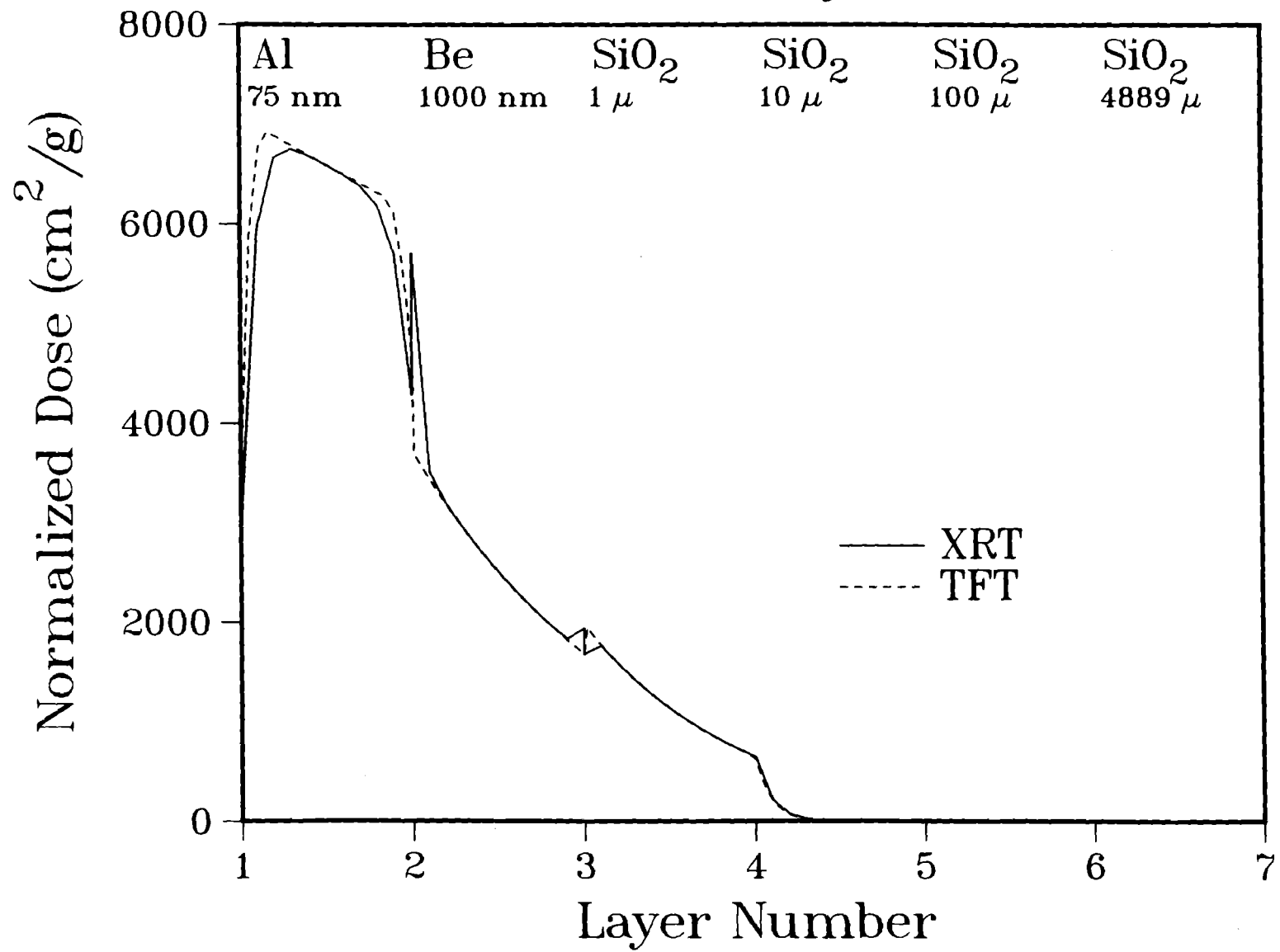
FIGURE 13

Mono–Energetic   20.0 keV
Without Secondary Effects
Except XRT and TART Include Fluorescence
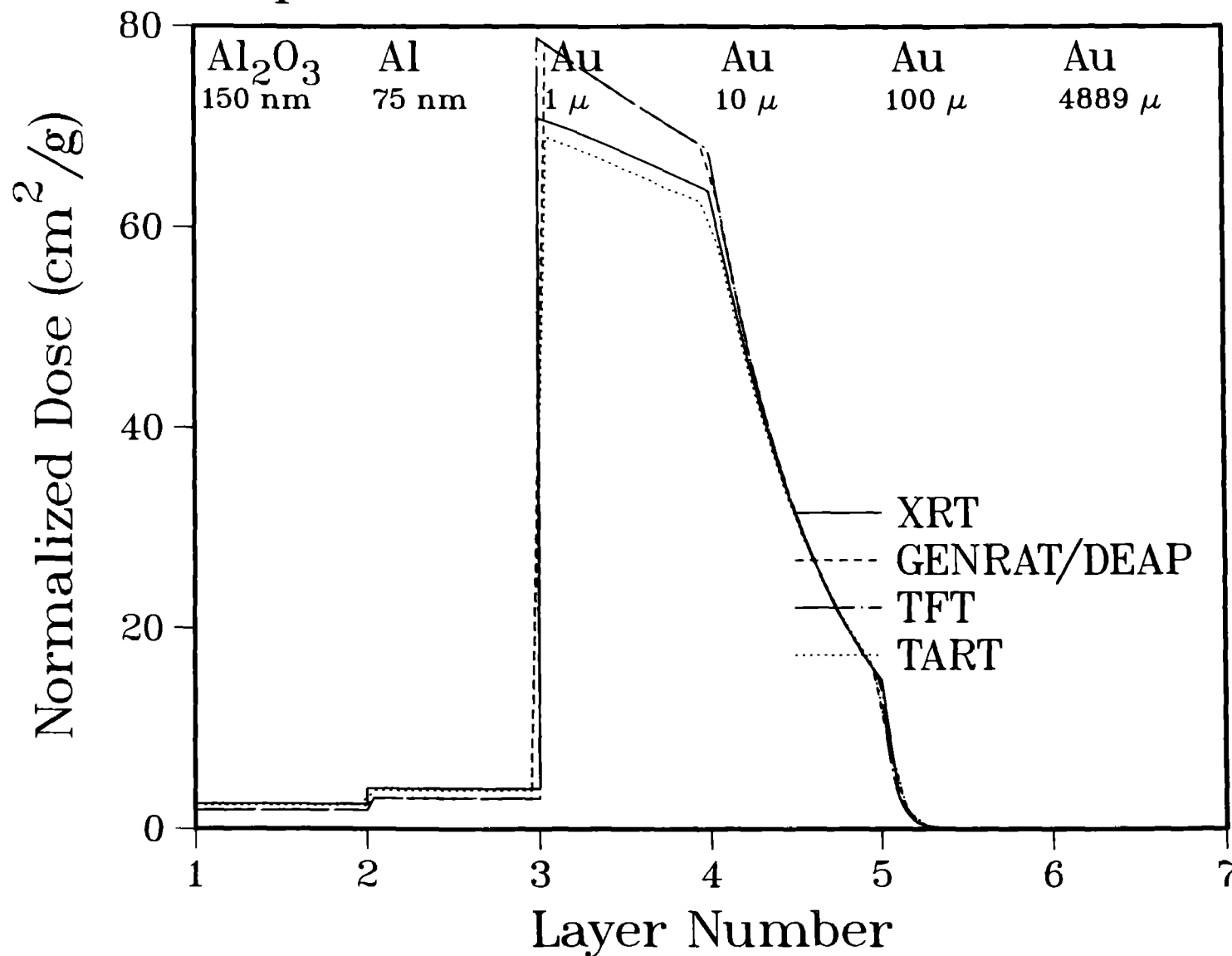
FIGURE 14

B4F

Mono−Energetic   20.0 keV
Without Secondary Effects
Except TART Includes Fluorescence

FIGURE 15

− 24 −
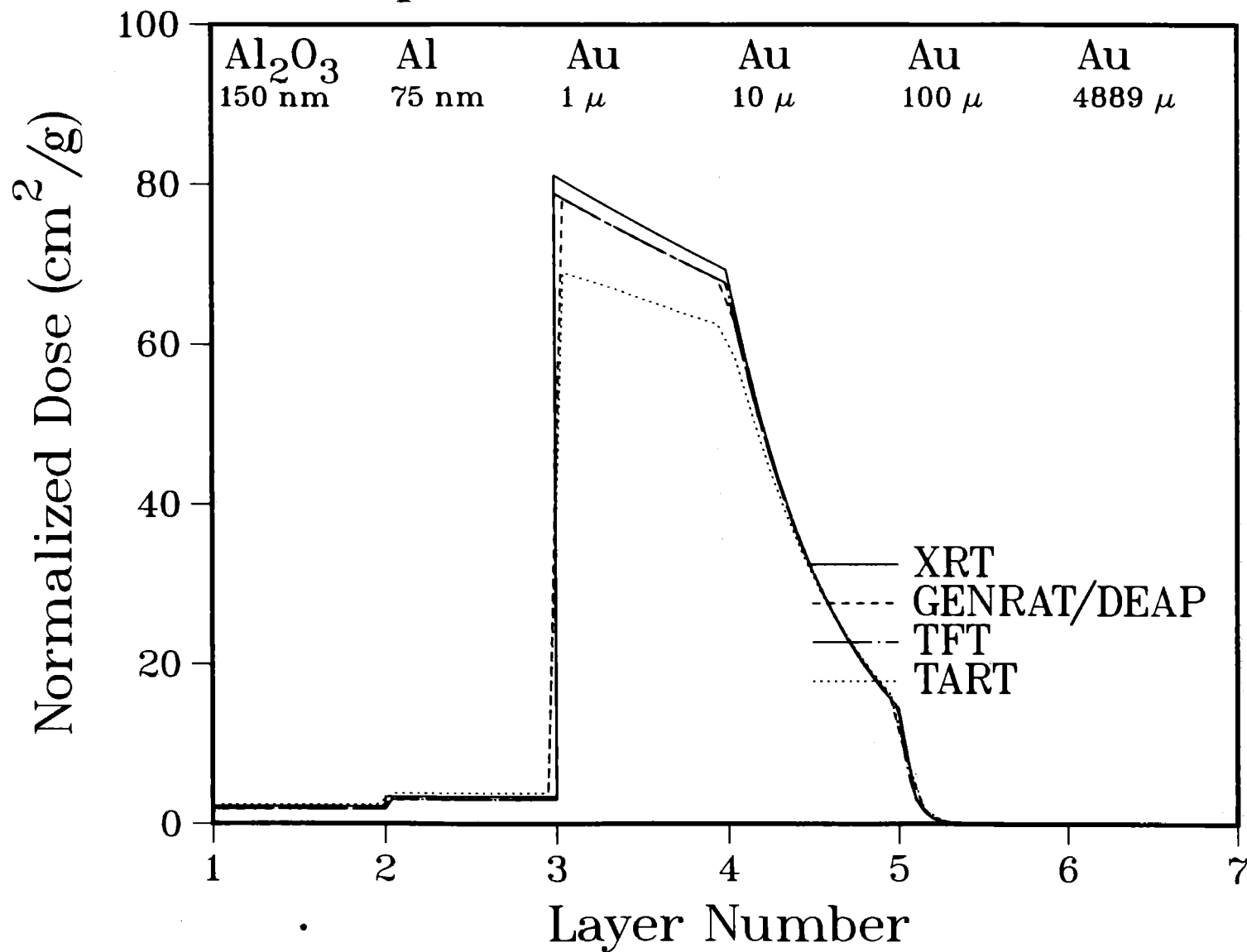
B4F   Mono-Energetic   20.0 keV

With Secondary Effects
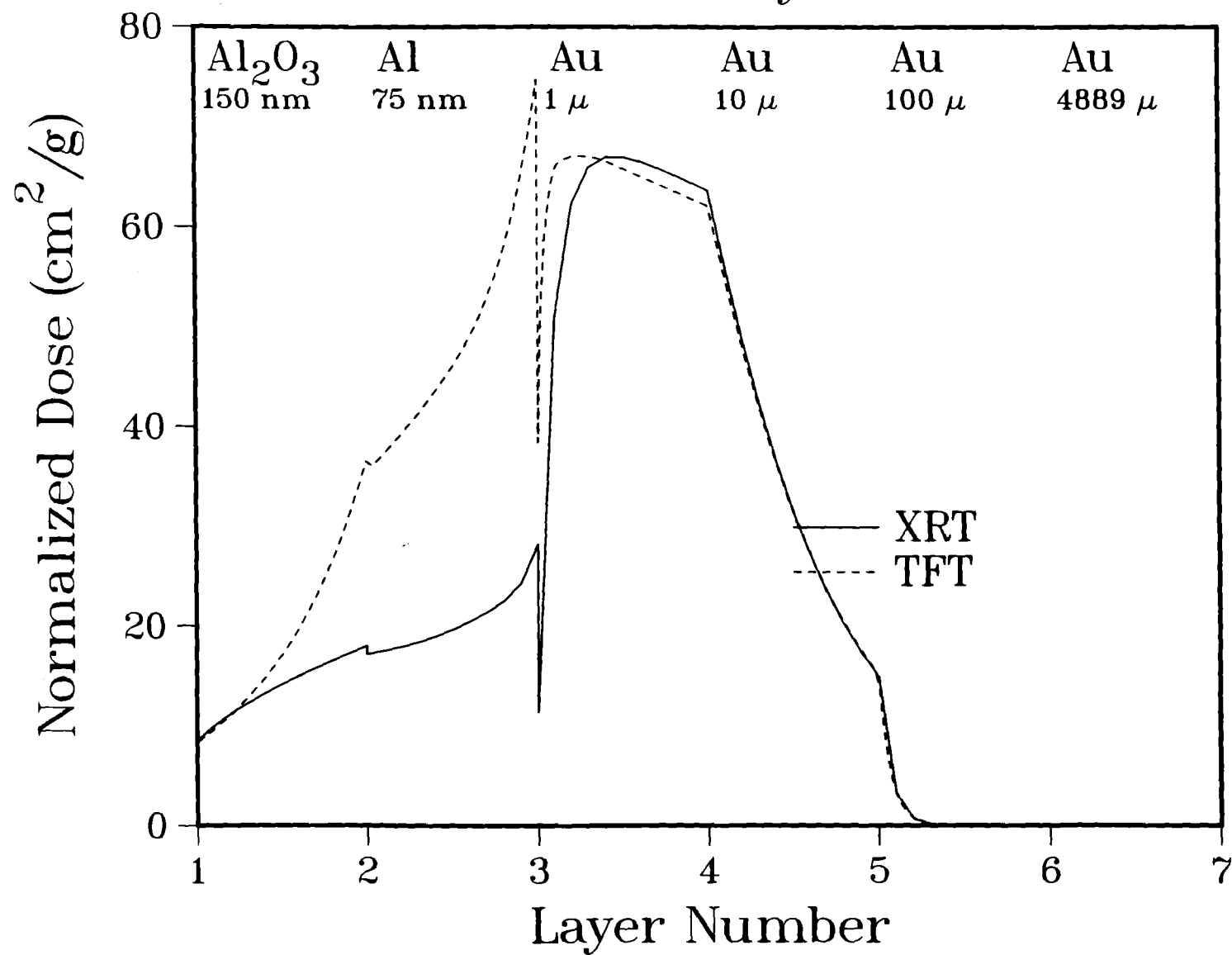
FIGURE 16
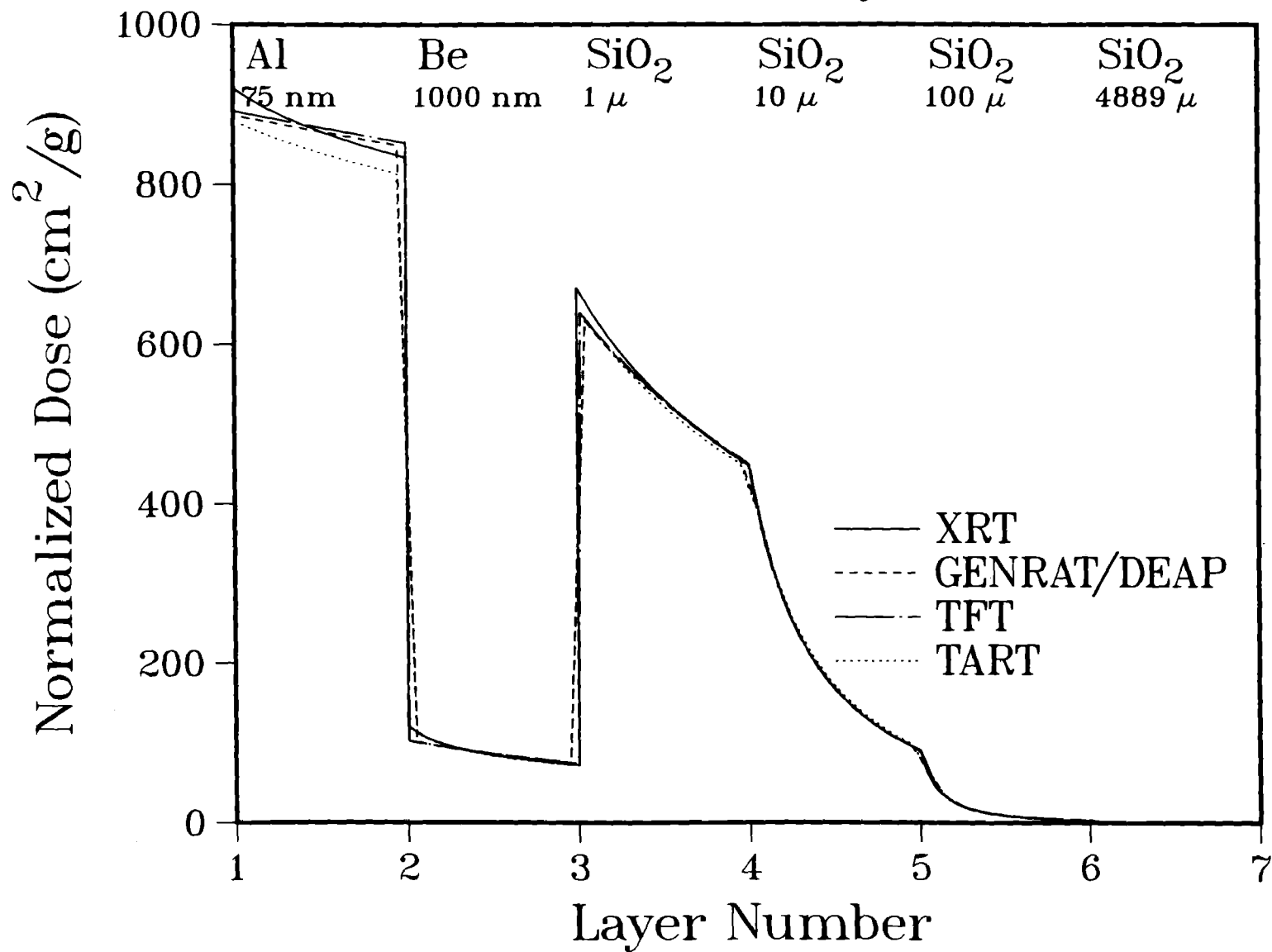
1 keV Blackbody

Without Secondary Effects

Al
75 nm

Be
1000 nm

SiO_2
1 μ

SiO_2
10 μ

SiO_2
100 μ

SiO_2
4889 μ

XRT
GENRAT/DEAP
TFT
TART

Normalized Dose (cm^2/g)

Layer Number

FIGURE 17

– 26 –

C1A

1 keV Blackbody
Fluence = 0.1 cal/cm^2 PD = 10 nsec
Without Secondary Effects

Enthalpy (cal/g) — End of Pulse

Al	Be	SiO$_2$	SiO$_2$	SiO$_2$	SiO$_2$
75 nm	1000 nm	1 μ	10 μ	100 μ	4889 μ

—— XRT
---- TFT

Layer Number
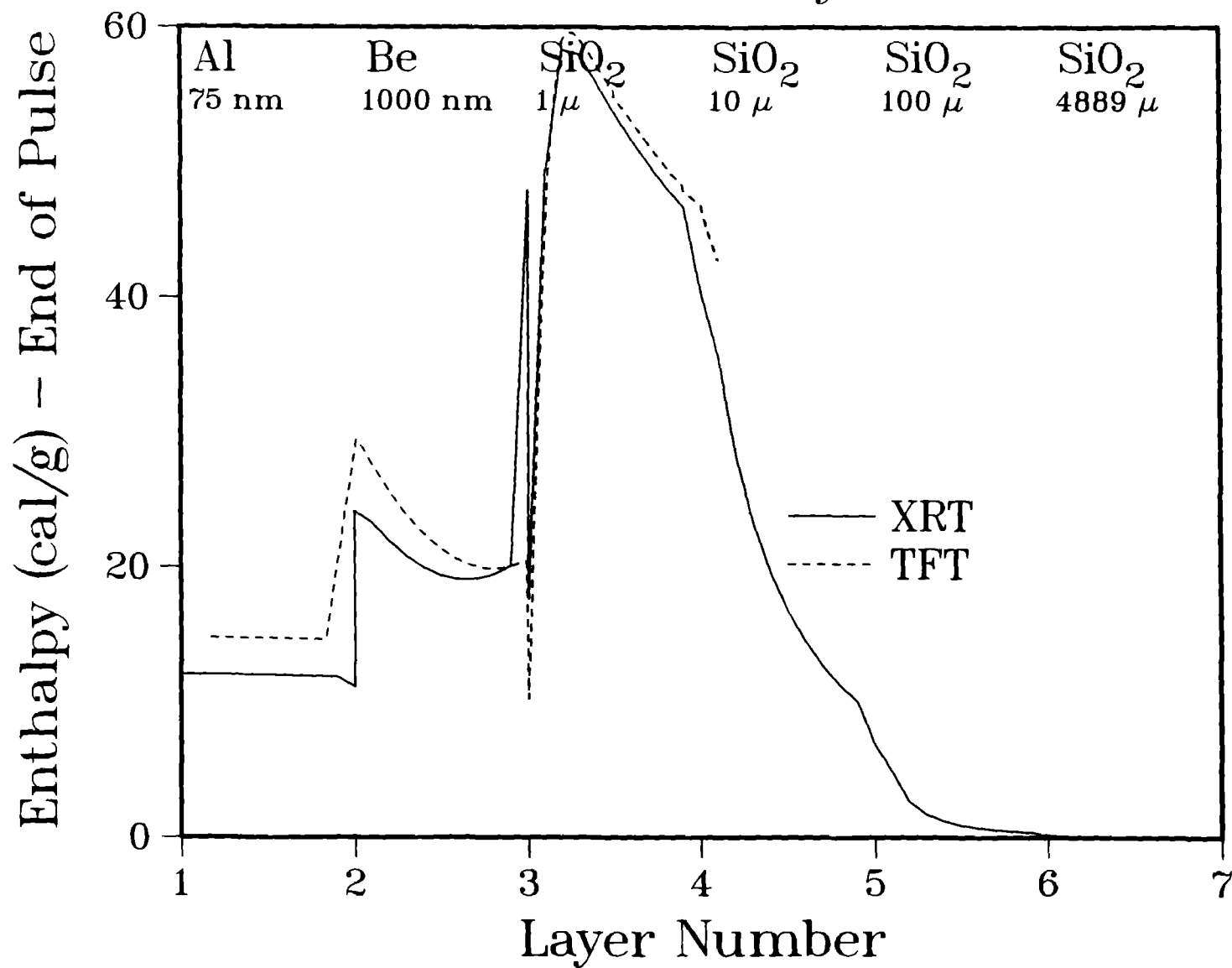
FIGURE 18

C1A

1 keV Blackbody
Fluence = 0.1 cal/cm^2 PD = 10 nsec
Without Secondary Effects
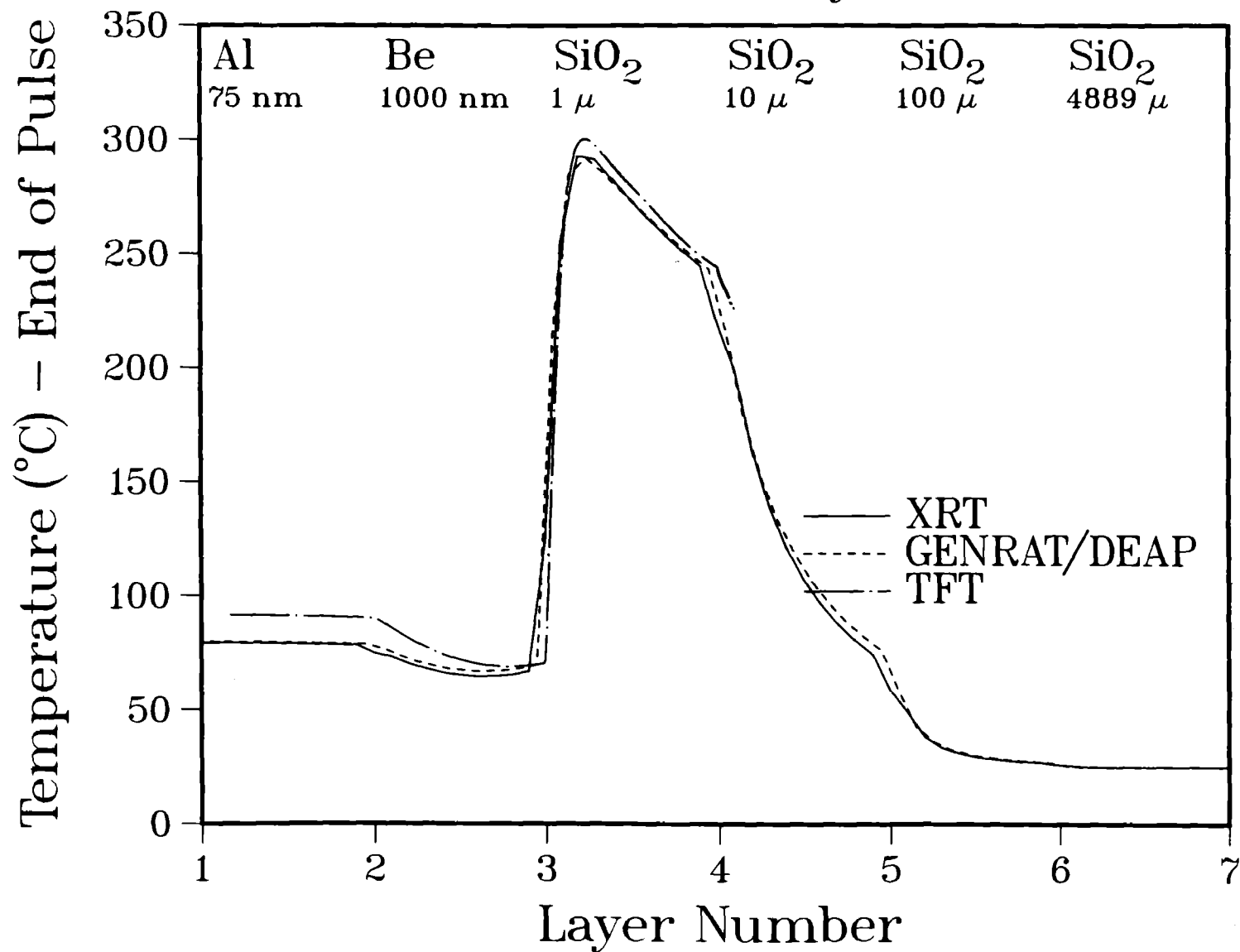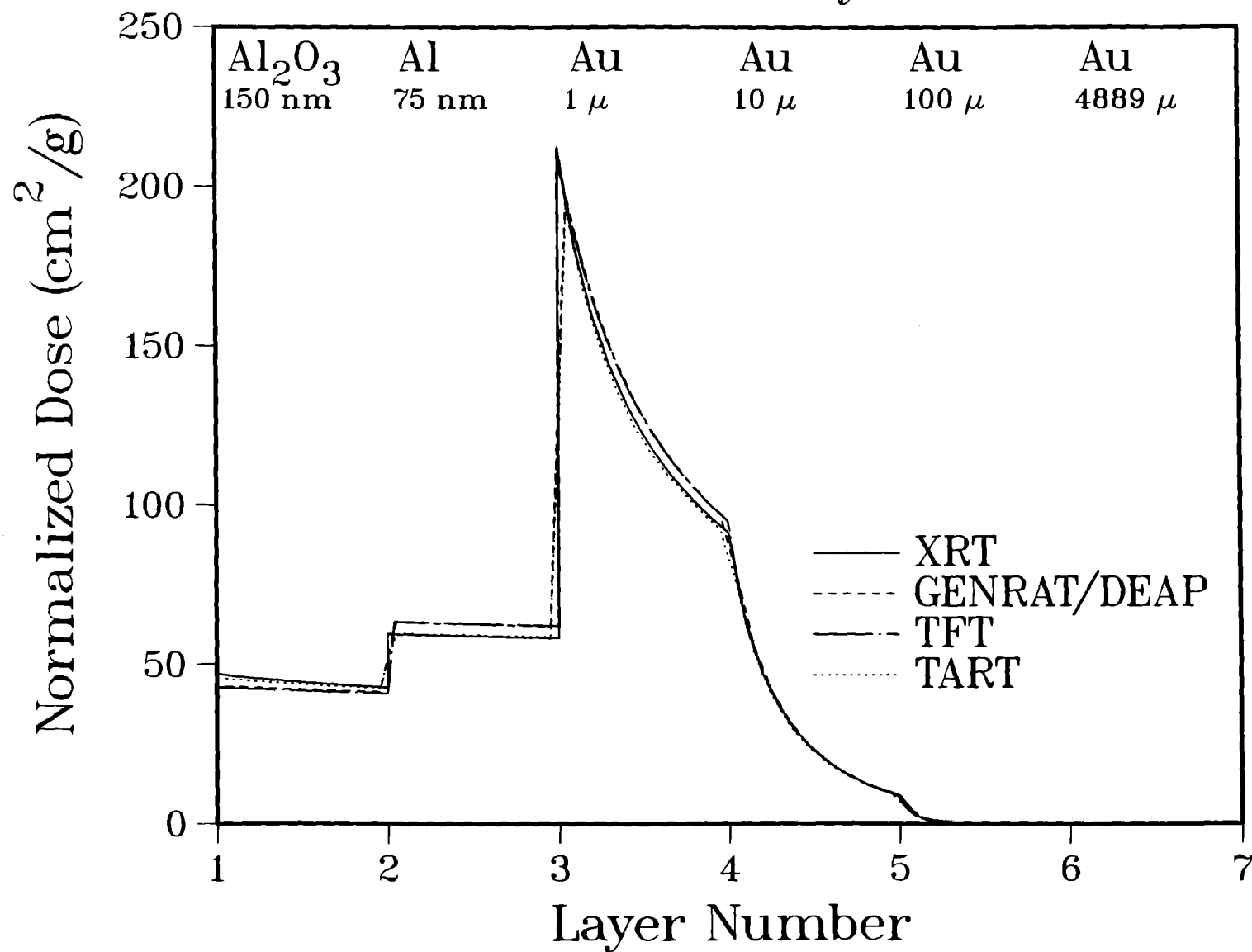
FIGURE 19

C1A

1 keV Blackbody

With Secondary Effects
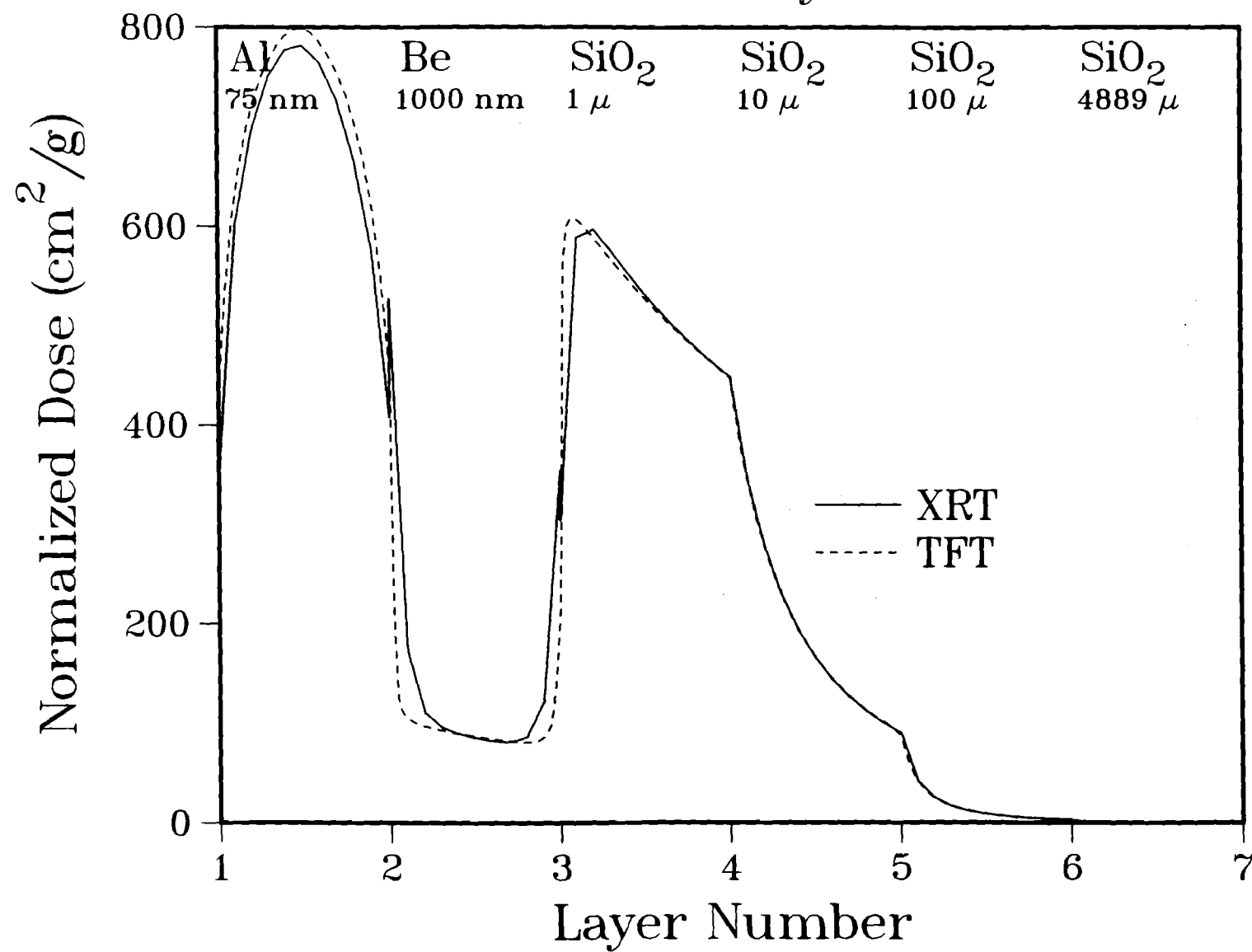
FIGURE 20

1 keV Blackbody
Fluence = 0.1 cal/cm^2 PD = 10 nsec
With Secondary Effects
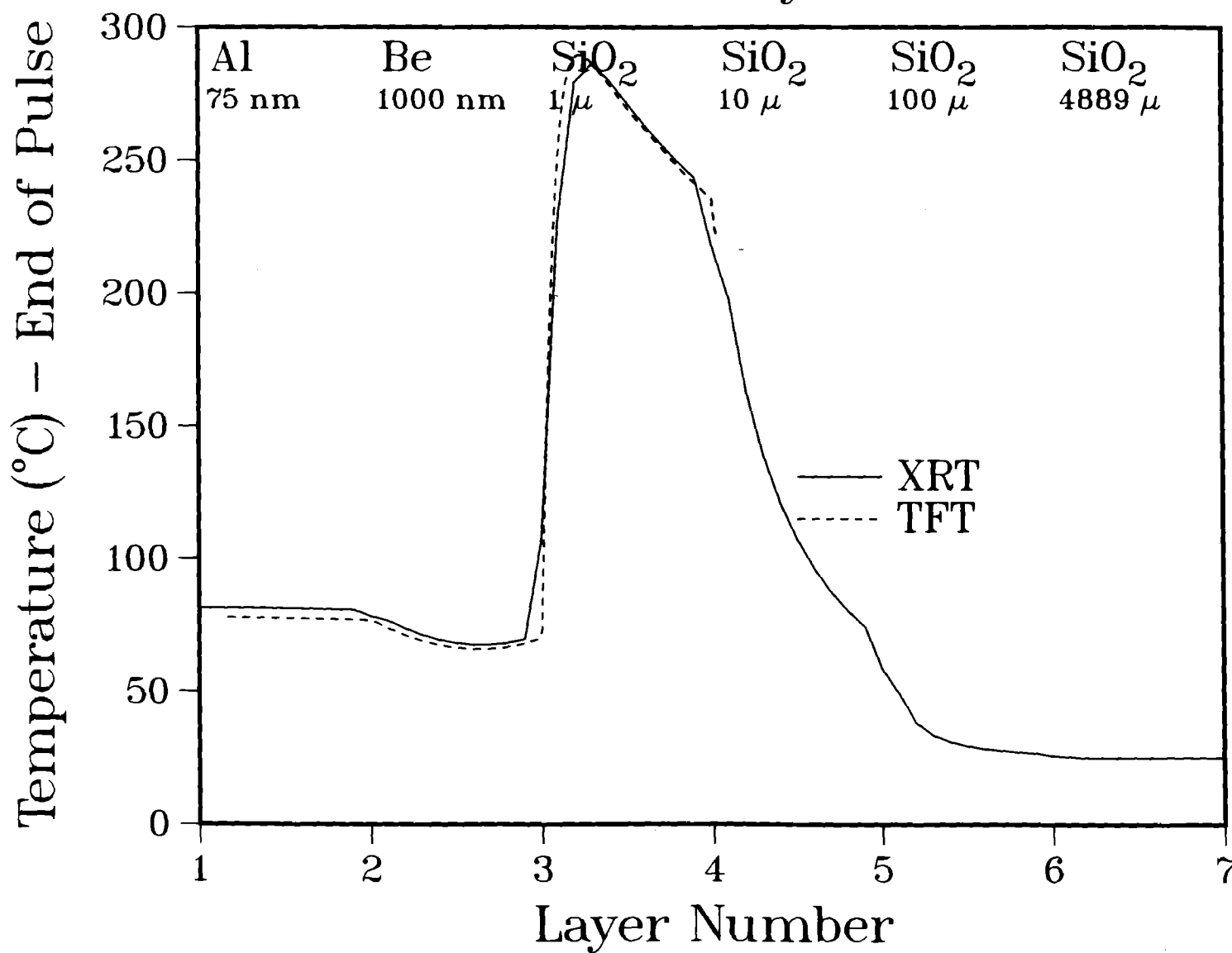
FIGURE 21

4 keV Blackbody

Without Secondary Effects

FIGURE 22

C4B

4 keV Blackbody
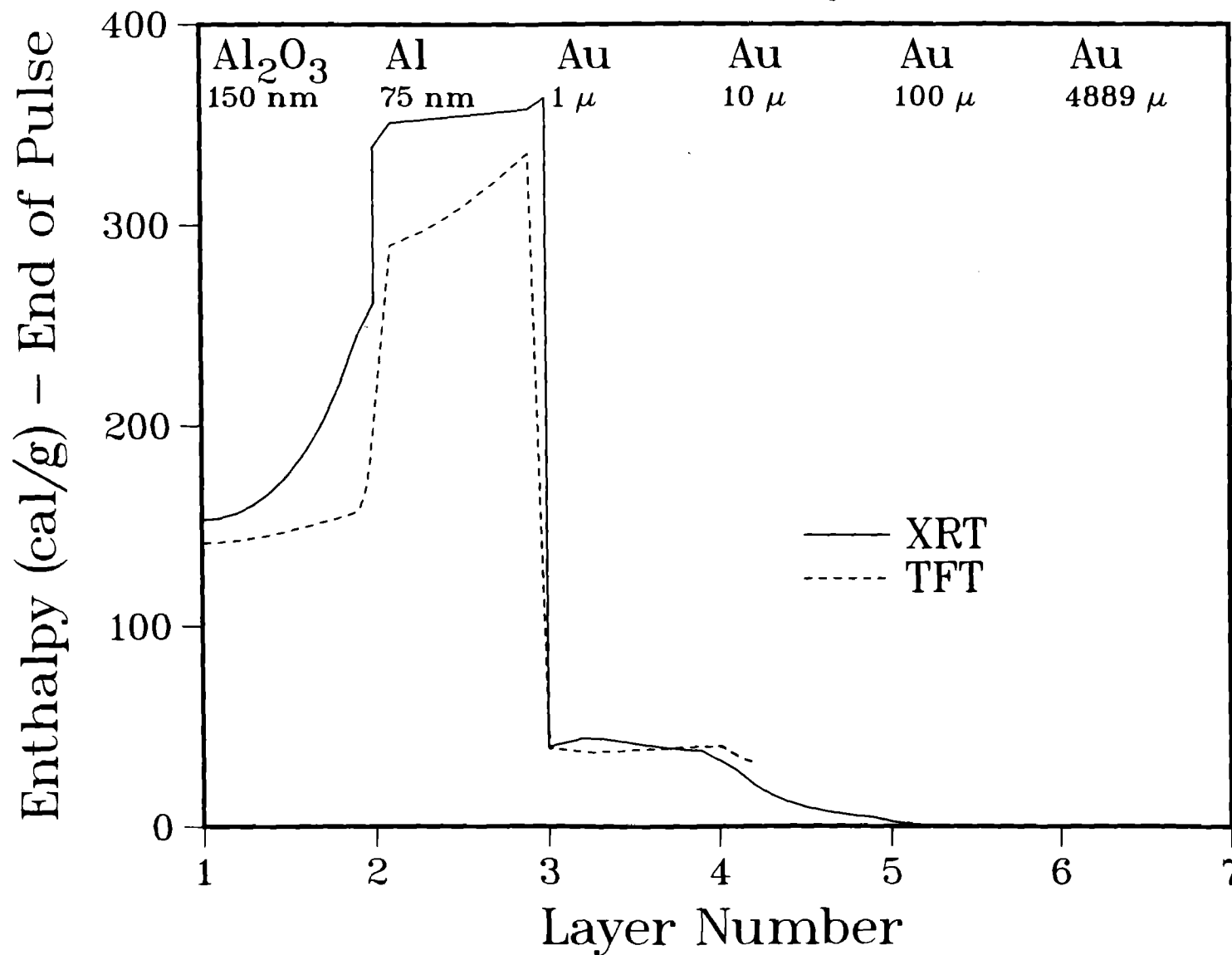Fluence = 0.4 cal/cm^2 PD = 10 nsec
Without Secondary Effects

FIGURE 23

C4B

4 keV Blackbody
Fluence = 0.4 cal/cm^2 PD = 10 nsec
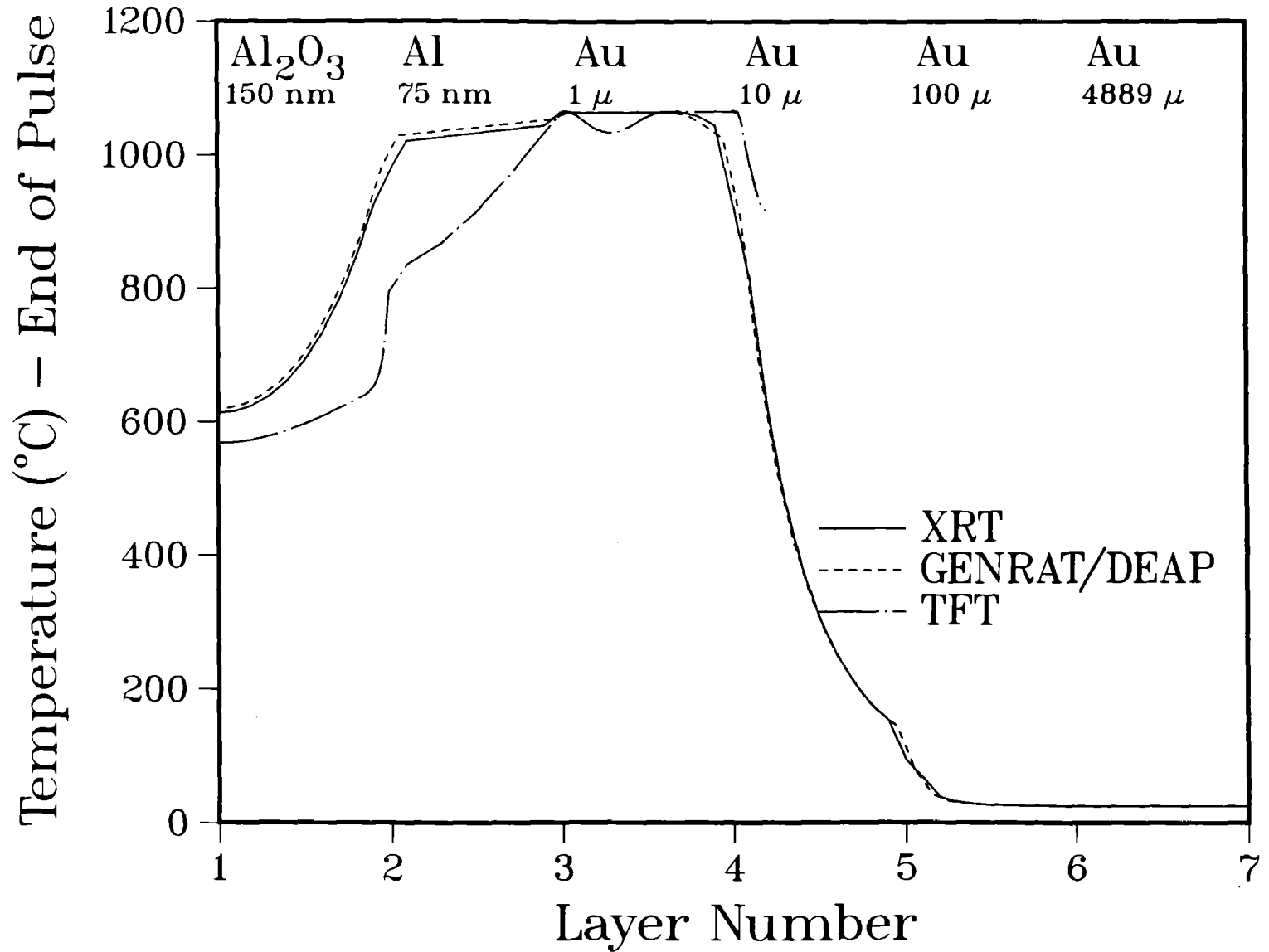Without Secondary Effects

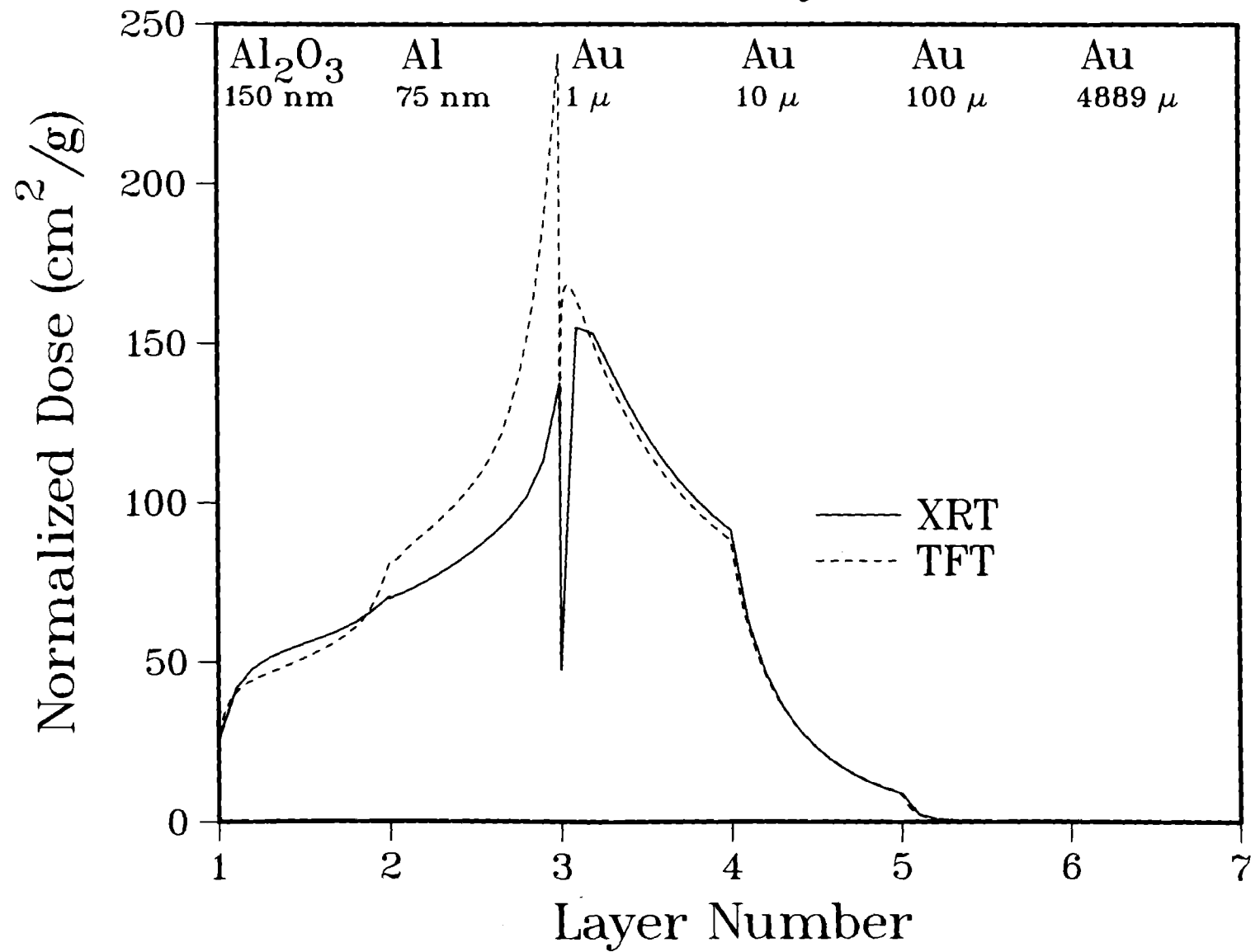FIGURE 24

4 keV Blackbody

With Secondary Effects

FIGURE 25

C4B

4 keV Blackbody
Fluence = 0.4 cal/cm^2 PD = 10 nsec
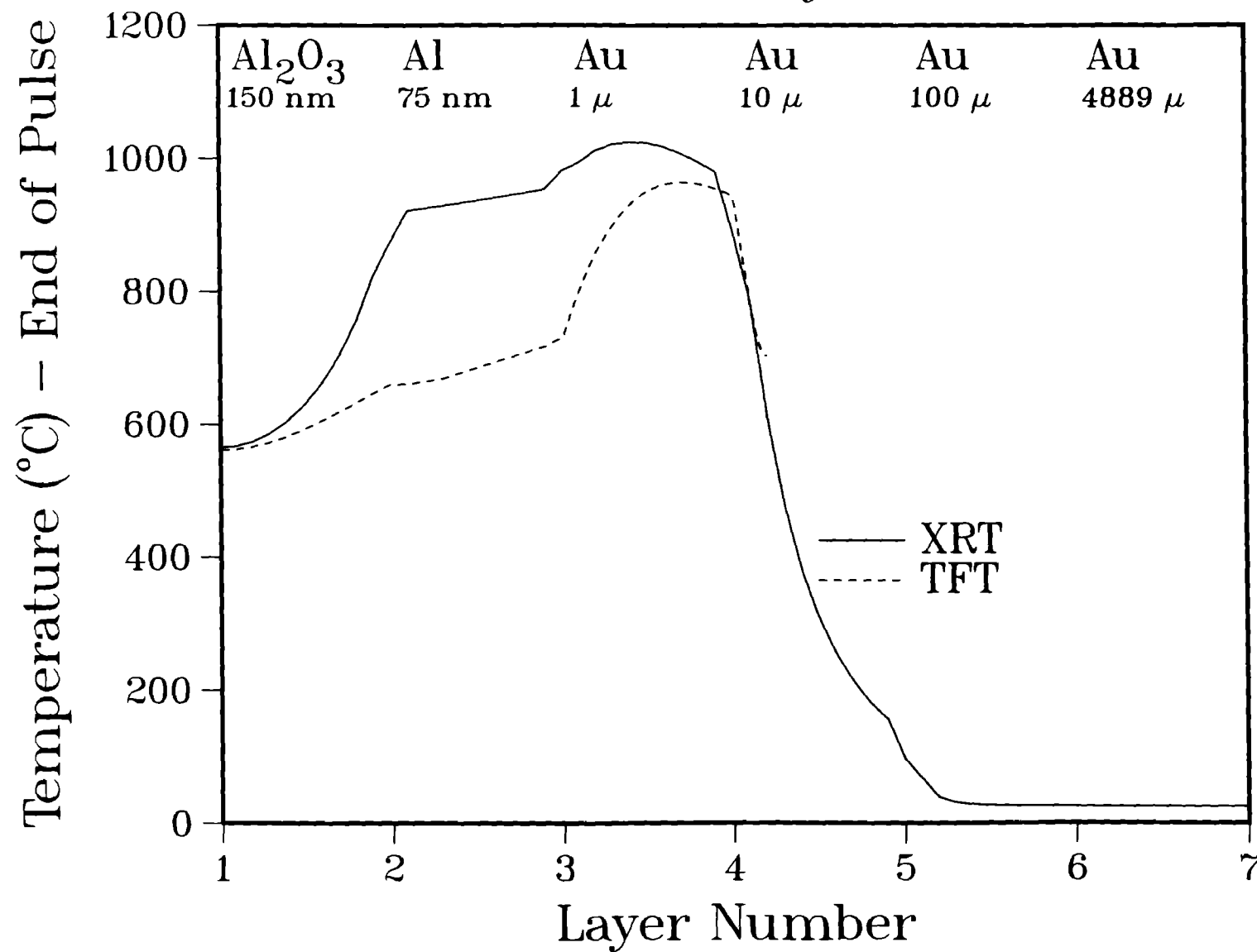With Secondary Effects

FIGURE 26

Argon
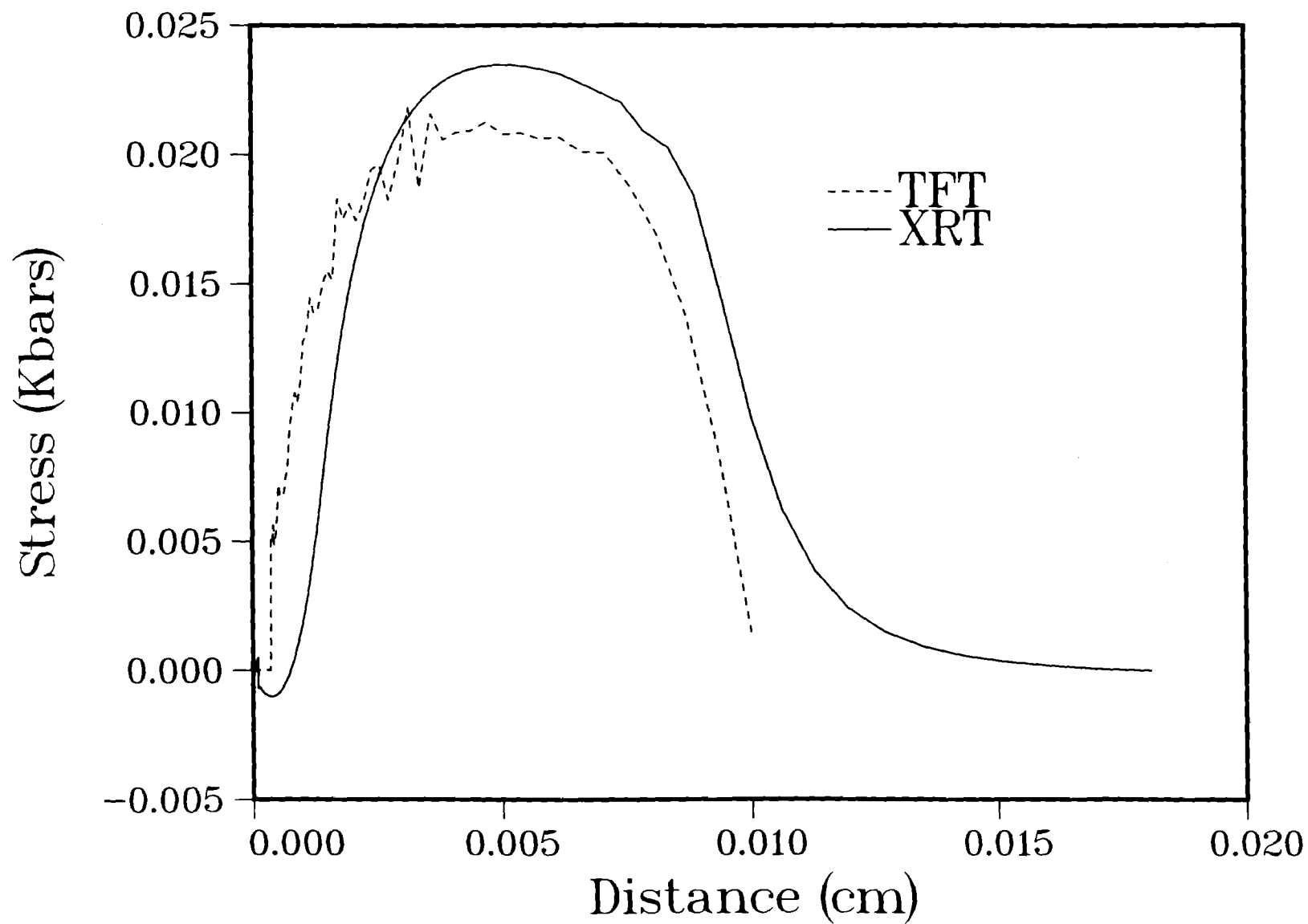Fluence = 0.9 cal/cm^2
TFT Time = 15.0 nsec
XRT Time = 17.0 nsec

Stress (Kbars)

Distance (cm)

FIGURE 27

Argon
Fluence = 0.9 cal/cm^2
TFT at 594 nm into SiO$_2$
XRT at 954 nm into SiO$_2$

A1A

FIGURE 28

– 37 –